Title

Resistant starch alters gut microbiome and metabolomic profiles concurrent with amelioration of chronic kidney disease in rats

Journal

American Journal of Physiology. Renal physiology, 310(9)

ISSN

0363-6127

Authors

Kieffer, Dorothy A
Piccolo, Brian D
Vaziri, Nosratola D
et al.

Publication Date

2016-05-01

DOI

10.1152/ajprenal.00513.2015

Peer reviewed

Articles in PresS. Am J Physiol Renal Physiol (February 3, 2016). doi:10.1152/ajprenal.00513.2015

Resistant Starch Alters Gut Microbiome and Metabolomics Profiles Concurrent with Amelioration of Chronic Kidney Disease in Rats

Dorothy A. Kieffer[1,2], Brian D. Piccolo[5], Nosratola D. Vaziri[3], Shuman Liu[3], Wei L. Lau[3], Mahyar Khazaeli[3], Sohrab Nazertehrani[3], Mary E. Moore[4], Maria L. Marco[4], Roy J. Martin[1], Sean H. Adams[2,5]

[1]Obesity & Metabolism Research Unit, United States Department of Agriculture-Agricultural Research Service Western Human Nutrition Research Center, Davis, CA; [2]Graduate Group in Nutritional Biology -and- Department of Nutrition, University of California, Davis; [3]Division of Nephrology, University of California, Irvine; [4]Department of Food Science and Technology, University of California, Davis; [5]Arkansas Children's Nutrition Center -and- Department of Pediatrics, University of Arkansas for Medical Sciences, Little Rock, AR

Corresponding author: Sean H. Adams, Arkansas Children's Nutrition Center, 15 Children's Way, Little Rock, AR 72202

Email: shadams@uams.edu

Telephone: 501-364-2785

Fax: 501-364-2818

Running title: Resistant Starch and Chronic Kidney Disease

Keywords: dietary fiber, resistant starch, chronic kidney disease, uremic retention solutes, gut microbiota

Abstract

Patients and animals with chronic kidney disease (CKD) exhibit profound alterations in the gut environment including shifts in microbial composition, increased fecal pH, and increased blood levels of gut microbe-derived metabolites (xeno-metabolites). The fermentable dietary fiber—high amylose maize resistant starch type 2 (HAMRS2)—has been shown to alter the gut milieu, and in CKD rat models leads to markedly improved kidney function. The aim of the current study was to identify specific cecal bacteria and cecal, blood, and urinary metabolites that associate with changes in kidney function, in order to identify potential mechanisms involved with CKD amelioration in response to dietary resistant starch. Male Sprague-Dawley rats with adenine induced CKD were fed a semi-purified low fiber or a high fiber diet (59% w/w of HAMRS2) for 3 weeks (n=9/grp). The cecal microbiome was characterized, and cecal contents, serum, and urine metabolites were analyzed. HAMRS2-fed rats displayed decreased cecal pH, decreased microbial diversity, and an increased Bacteroidetes to Firmicutes ratio. Several URS solutes were altered in the cecal contents, serum, and urine, many of which had strong correlations with specific gut bacteria abundances: i.e., serum and urine indoxyl sulfate were reduced by 36% and 66%, respectively in HAMRS2-fed rats, and urine p-cresol was reduced by 47% in HAMRS2-fed rats. Outcomes from this study were coincident with improvements in kidney function indices and amelioration of CKD outcomes previously reported for these rats, suggesting an important role for microbial-derived factors and gut microbe metabolism in regulating host kidney function.

Introduction

Patients and animal models with CKD exhibit an altered gut microbiota and increased gut permeability (52, 76, 78, 79). These changes in gut milieu may occur for several reasons, including diet (i.e., decreased dietary fiber intake), prolongation of intestinal transit time, and influx of uremic retention solutes (30) from the systemic circulation into the colonic lumen. URS are metabolites that accumulate in the blood and tissues of CKD patients and animal models due to the decline in the number of functioning nephrons (68, 72). In CKD patients the concentration of urea in the intestinal fluids is similar to its serum concentration. Urea, at concentrations found in stable end-stage renal disease (ESRD) patients, has been shown to significantly reduce the epithelial tight junction proteins in human colonocytes. The damaging effect of urea was greatly amplified in the presence of urease, an enzyme that is abundantly expressed by numerous gut microbial species (77). Earlier studies by the Vaziri lab have shown marked alterations of the gut microbiome in rats and humans with advanced CKD (75). The CKD-induced changes in the gut microbiome were characterized by expansion of microbial families possessing genes encoding urease, uricase, indole and *p*-cresol metabolizing enzymes, and depletion of microbes expressing short chain fatty acid-forming enzymes (85).

Patients with CKD are often advised to limit their consumption of fiber-rich foods that are high in potassium and phosphorus, to prevent cardiac arrhythmias and bone mineral disorders, respectively (1, 56). This is, however, of potential concern since decreased dietary fiber intake can also increase gut permeability (21, 23, 24), which in theory could increase the blood exposure to gut-derived URS or other factors that impact kidney function and inflammation. Low fiber diets promote the growth of bacteria that consume host glycans, leading to degradation of the protective mucus barrier lining of the intestinal epithelia and thereby facilitate translocation of luminal contents, such as bacteria and their noxious products/components, into

the intestinal wall and systemic circulation (17, 63, 64, 79). Indeed, patients with CKD often display elevated blood levels of the microbial-modified amino acids indoxyl sulfate and *p*-cresol sulfate. The rise in these URS is attributed to reduced renal elimination (55), however it is not known at this time to what extent, if any, other factors such as increased gut permeability, changes in intestinal transport and/or increased microbial production may also contribute to increased circulating levels. These URS metabolites are known to promote inflammation and increase the risk of cardiovascular disease (6, 41, 73). Interestingly, dietary fibers have been shown to improve kidney function and decrease levels of these potentially harmful metabolites (47, 60).

One dietary fiber shown to decrease nitrogenous and microbial-derived URS is high-amylose maize resistant starch type 2 (HAMRS2) (60, 74). HAMRS2 is derived from corn that has been naturally selected to contain a higher amylose:amylopectin ratio. The linear amylose molecules form granules that partially resist digestion by mammalian enzymes in the small intestine. The remaining approximately 60% of undigested HAMRS2 passes into the large intestine where it can be fermented by microbes (3). In animal models, HAMRS2 increased fecal nitrogen excretion, lowered plasma urea and altered gut bacterial communities (16, 32, 87). Using the adenine-induced CKD rat model, we recently reported that 3 weeks of dietary HAMRS2 (59% by weight of the diet) led to significant improvements in kidney histology and kidney function (74). Based on these observations, we set out to identify specific cecal bacteria and cecal, blood, and urinary metabolites that associate with changes in kidney function, in order to identify potential mechanisms involved with CKD amelioration in response to dietary resistant starch.

Materials and Methods

Animals and Diets

Animals, housing conditions, and diets have been previously described (74). Briefly, 10 week old male Sprague-Dawley rats (Harlan Laboratories, Indianapolis, IN) were fed powdered chow (Harlan, 2020X) containing 0.7% adenine for 2 weeks to induce a CKD-like phenotype. Rats were then randomized to receive semi-purified pelleted diets supplemented (59% by weight) with either the rapidly digestible starch amylopectin (low fiber) or HAMRS2 (Hi-Maize 260, Ingredion, Westchester, IL) for 3 weeks (n=9/group). Isocaloric diets were prepared by Harlan Laboratories (Madison, WI) and had an energy content of 14.5%/66.9%/18.6% protein/carbohydrate/fat, respectively. All animals were provided *ad libitium* access to food and water. Rats were placed in metabolic cages for 24 hour urine collection. On the day of tissue harvest, *ad libitum*-fed rats were anesthetized (ketamine, 50 mg/kg plus xylazine, 4 mg/kg IP) and euthanized via cardiac exsanguination, between ca. 08:00-11:00. Blood was collected and left at room temperature for 30 minutes to clot, serum was collected, frozen on dry ice and stored at -70˚C until processing. Cecal contents were removed and frozen on dry ice and stored at -70˚C until processing. Hydration of cecal contents was determined by weighing a frozen aliquot, then oven drying overnight at 100˚C, allowed to cool, and weighed twice to ensure a constant weight was obtained. All experiments were approved by the University of California Irvine Institutional Committee for the Use and Care of Experimental Animals.

pH of cecal contents

Cecal contents were thawed on ice and approximately 400 mg of cecal contents was transferred to a clean tube and HPLC grade water was added at a 10:1 ratio, homogenized for 2 minutes at 1200 rpm on a Geno/Grinder, then centrifuged for 10 min at 4˚C at 3509 g (Sorvall Legend X1R). A Corning 320 pH meter was used to determine pH of the cecal water.

Metabolomics

Details of this procedure have been previously published for serum or plasma (19). Untargeted primary metabolite analysis (i.e. sugars, amino acids, nucleotides and their derivatives) of cecal contents, serum, and urine was performed on all 9 rats in each group at the West Coast Metabolomics Center (http://metabolomics.ucdavis.edu/) using GC-TOF-MS. For serum and urine, 15 µL was added to 1 mL of ice-chilled extraction solution (acetonitrile:isopropanol:water, 3:3:2) and vortexed for 10 seconds. This same procedure was conducted using an approximately 10 mg sample of frozen cecal contents. Samples were centrifuged for 2 minutes at 14,000 g (Eppendorf 5415D), 500 µL of supernatant was evaporated (Labconco Centrivap) to complete dryness. For derivitization, 10 µL of methoxyamine hydrochloride (Aldrich) was added to dried samples and left on a shaker for 90 minutes at 30˚C, and then 91 µL of 100:1 N-methyl-N-(trimethylsilyl)-trifluoroacetamide (Aldrich): fatty acid methyl ester mixture was added. Samples were left on shaker for 30 minutes at 37˚C.

Analyses were performed using an Agilent 6890 GC equipped with a Gerstel automatic liner exchange system that includes a multipurpose sample (MPS2) dual rail, and a Gerstel CIS cold injection system (Gerstel, Muehlheim, Germany) with the temperature ramp: 50°C to 275°C final temperature at a rate of 12 °C/s, and held for 3 minutes. Injection volume was 0.5 µL with 10 µL/s injection speed on a splitless injector with purge time of 25 seconds. The liner (Gerstel #011711-010-00) was changed after every 10 samples. Before and after each injection, the 10 µL injection syringe was washed three times with 10 µL ethyl acetate. Gas Chromatography conditions: A 30 m long, 0.25 mm i.d. Rtx-5Sil MS column (0.25 µm 95% dimethyl 5% diphenyl polysiloxane film) with additional 10 m integrated guard column was used (Restek, Bellefonte PA). Helium (99.9999% purity) with built-in purifier (Airgas, Radnor PA) was set at constant flow of 1 mL/min. The oven temperature was held constant at 50°C for 1 min and then ramped at 20°C/min to 330°C at which it was held constant for 5 min.

Mass spectrometer settings and data acquisition: A Leco Pegasus IV time of flight mass spectrometer was used, controlled by the Leco ChromaTOF software vs. 2.32 (St. Joseph, MI). The transfer line temperature between gas chromatograph and mass spectrometer was set to 280°C. Electron impact ionization at 70V was employed with an ion source temperature of 250°C. Acquisition rate was 17 spectra/second, with a scan mass range of 85-500 Da. Result files were exported to servers and processed by the Fiehn lab metabolomics database, known as BinBase (20). Database entries in BinBase were matched against the Fiehn mass spectral library of 1,200 authentic metabolite spectra using retention index and mass spectrum information or the NIST05 commercial library. Identified metabolites were reported if present in at least 50% of the samples, regardless of treatment group (as defined in the SetupX database) (58). Each metabolite was normalized by the sum of identified metabolite quantifier ion peak heights (QIPH) present in each individual sample. These relative abundances were used for subsequent statistical analysis. Cecal-derived metabolite abundances were corrected for dry weight by dividing the metabolite abundance by percent dry matter obtained by oven drying as described above.

Cecal Microbiota

Total cecal DNA was extracted by bead beating with 0.1 mm zirconia/silica beads (BioSpec) followed by DNA purification using the QIAamp DNA stool mini kit (Qiagen Inc., Valencia, CA). Twenty ng/μL of DNA was used to amplify the V4 region of the 16S rRNA gene with 30 PCR cycles at 94˚C for 45 seconds, 54˚C for 60 seconds, and 72˚C for 30 seconds using barcoded 515 forward (5'-GTGCCAGCMGCCGCGGTAA-3') and 806 reverse (5'-GGACTACHVGGGTWTCTAAT-3') primers (12). Equal molar amounts of PCR amplicons were then pooled and gel purified using Wizard SV Gel and PCR clean-up system (Promega Corporation, Madison, WI). Sequencing of pooled 250-bp paired-end amplicons was performed with an Illumina MiSeq (San Diego, CA) at the UC Davis Genome Center

(http://dnatech.genomecenter.ucdavis.edu). Raw Illumina FASTQ files were de-multiplexed and quality filtered with Quantitative Insights Into Microbial Ecology software (QIIME Version 1.8.0) (11). Assembled reads were used for Operational Taxonomic Unit (OTU) picking. OTUs sharing at least 97% nucleotide identity were identified using an open-reference OTU picking process according to a 16S rRNA sequence database, Greengenes version 13_8 and further analyzed in QIIME.

Statistical Analysis

Statistical analyses were performed using GraphPad Prism (Version 5.04 for Windows, GraphPad Software, San Diego, CA) or R version 3.1.2 (51). Dietary related differences in cecal hydration, cecal tissue weight, cecal pH and number of cecal microbial species were assessed with a two-tailed unpaired Student's *t*-test. Bacterial percent abundance data expressed as mean percent abundance and group differences were assessed with Mann-Whitney U tests. Group comparison of all metabolomics data were assessed by Mann-Whitney U tests. Results from univariate comparisons were adjusted to account for the false discovery rate (FDR) using the Benjamini and Hochberg (8) and statistical significance was considered at $\alpha = 0.05$. Multivariate analysis of metabolomics data was performed using partial least squares-discriminate analysis (PLS-DA) from the R package "pls" (45). PLS-DA was utilized due to its ability to reduce the dimensionality of the data while maximizing the variance between the dependent and exploratory variables. Data used in PLS-DA models were assessed for univariate outliers using Grubb's test with the R package "outliers" (34). Outliers were removed if determined to be significant at $\alpha = 0.01$. In total, 95 outliers were removed; which accounted for 0.4% of the entire metabolomics data. Removed outliers were imputed using k nearest neighbors from the Bioconducter "impute" package (27). PLS-DA model accuracy was assessed with a cross-validation scheme where the data were randomly partitioned into training and test datasets encompassing 2/3 (n=6/grp) and 1/3 (n=3/grp) of all animals, respectively.

Training data were scaled and centered to unit variance prior to model development, while test data were scaled and centered using the means and standard deviations from the training data. Metabolites of interest were identified with training data using variable importance in projection (VIP) measurements from bootstrapped PLS-DA models. VIP is a weighted measure of the contribution of each metabolite to discriminate the classification groups (low fiber vs. HAMRS2). A VIP score of ≥ 1 has been argued as an adequate threshold to determine discriminant variables in the PLS-DA model (40, 83); therefore, we used this criterion as a cutoff to assess which metabolites provide discriminate information in the models. Metabolites that had a bootstrapped VIP ≥ 1 and an FDR corrected MWU p-value ≤ 0.05 were chosen for inclusion in final PLS-DA models. Model performance was assessed based on the model's ability to accurately predict the classification of the test set animals using data from the training set. Final models were able to predict the classification of the test set animals with 100% accuracy. Variance explaining group classification related to dietary differences were visualized in scores plots using scores from the first two dimensions in PLS-DA models. In these scores plots, each symbol represents a single rat and group membership are represented by shape and color. Group confidence regions are represented by ellipses based on 95% confidence intervals determined by Hotelling's T^2. Rats whose symbols are closer to one another have a more similar metabolite profile, whereas rats with larger distances from each other have dissimilar metabolite profiles. Principal Component Analysis (PCA) scores plots from rats used in the validation model can be found in **Figure 1**. Metabolites used to generate these plots were the same that were used to generate the PLS-DA scores plots for serum, urine, and cecal metabolites. PCA is an unsupervised multivariate analysis, meaning that the model is generated without information regarding treatment groups.

Results

Our previous publication described kidney function, renal histopathology, renal expression of inflammatory, oxidative, and fibrosis pathway proteins, as well as colonic tight junction protein levels in this cohort of CKD rats (74). Briefly, supplementation with HAMRS2 markedly improved kidney function and gut permeability indices: i.e., decreased serum creatinine, increased creatinine clearance, improved tubulo-interstitial injury score, decreased kidney protein levels of inflammatory proteins (i.e. NF-kB, MCP-1, COX-1, TGF-β), increased kidney protein levels of endogenous antioxidants (i.e. CuZn SOD, catalase, glutathione peroxidase) and restored colonic tight junction proteins (occludin and claudin-1). No changes in body weight were observed. The focus of the current research was to explore the effect HAMRS2 on metabolite and microbiome patterns, and their possible association with the observed improvements in kidney function in rats with CKD.

HAMRS2 significantly altered cecal milieu and microbiota

Cecal characteristics and bacterial phyla summary are depicted in **Table 1**. The cecal contents of HAMRS2-supplemented rats were significantly more hydrated than low fiber-fed rats; this is consistent with fecal hydration data previously reported for these animals (74). Cecal tissue weight was significantly greater and cecal content pH was significantly reduced in the HAMRS2 fed rats. Rats consuming HAMRS2 harbored a distinct cecal microbiota compared to those fed the low fiber diet, as indicated by Principal Coordinates Analysis (PCoA) of the unweighted UniFrac metric (42), for which 44% of the variation in bacterial composition could be explained by the inclusion of HAMRS2 in the diet (see separation along the PC1 dimension, **Figure 2A**). There were, on average, 15% fewer observed bacterial species in the cecum of the HAMRS2 group. Detailed bacterial abundance data can be found in **Supplemental Table S1**. The relative abundances of *Actinobacteria* and *Proteobacteria* were significantly greater, and *Firmicutes* were significantly reduced, in the HAMRS2-fed rats

compared to low fiber-fed rats. HAMRS2-fed rat ceca contained a 66% higher ratio of Bacteroidetes to Firmicutes (B:F) when compared to the low fiber-fed rats despite no significant difference in the proportions of Bacteroidetes between groups (**Table 1**).

Percent changes of select bacteria in HAMRS2-fed CKD rats relative to low fiber CKD controls are shown in **Figure 2B**. Within the Actinobacteria phylum, proportions of the genus *Bifidobacterium* were significantly greater in the HAMRS2-fed rats which had an average relative abundance of 1.11% compared to low fiber-fed rats which had 0.62% ($p=0.002$). Within the Bacteroidetes phylum, proportions of the family Barnesiellaceae were greater in the HAMRS2-fed rats compared to low fiber-fed rats, at 0.30% vs. 0.15%, respectively ($p=0.0003$). The HAMRS2 rats also had greater proportions of the Bacteroidetes family S24-7 compared to the low fiber group, with 9.75% and 3.58% abundance, respectively ($p=0.0003$). Conversely, the Bacteroidetes genus *Prevotella* was reduced in the HAMRS2-fed rats compared to low fiber-fed rats, with 0.11% and 0.05%, respectively ($p=0.0004$). Although the total numbers of bacteria within the Firmicutes phylum declined with HAMRS2 consumption, there were strikingly higher proportions of bacteria within the genus *Allobaculum*, with 0.56% relative abundance in the low fiber group and 15.43% in the HAMRS2-fed rats ($p=0.003$). Similarly, *Faecalibacterium* also had greater proportions in the HAMRS2 group with 0.84% compared to 0.71% in the low fiber group ($p<0.05$). *Ruminococcus*, another genus within the Firmicutes, was higher in the HAMRS2 group with 21.27% compared to 5.86% in the low fiber group ($p=0.0003$). The following Proteobacteria proportions were significantly enriched in rats fed HAMRS2: order RF32 (Alphaproteobacteria), genus *Sutterella* (Betaproteobacteria), family Enterobacteraceae (Gammaproteobacteria). There was a significant reduction in the family Desulfovibrionaceae (Deltaproteobacteria) in the HAMRS2 fed rats compared to the low fiber group.

HAMRS2 significantly alters cecal, serum, and urine metabolite profiles

Partial least squares-discriminant analysis (PLS-DA) scores plots for metabolomics results in cecal contents, serum, and urine of rats used for statistical model generation are shown in **Figure 3.** In these plots, it is readily apparent that variance in selected metabolites can discriminate rats in the low fiber group compared to the HAMRS2 group. Annotated metabolites that were featured in PLS-DA models are listed in **Tables 2-4** (note that non-annotated metabolites are not listed, for brevity). A general pattern of metabolite changes in the cecal contents, serum, and urine is presented in **Table 6**. All of the metabolomics data including non-annotated and annotated metabolites identified in cecal contents, serum, and urine can be found in **Supplemental Table S2**.

Cecal Metabolites

A total of 465 cecal metabolites were detected using the GC-TOF analytical platform. Of these, 202 metabolites were annotated in the metabolite database; the remaining metabolites were non-annotated and labeled with a numerical BinBase ID (**Supplemental Table S2A**). A total of 256 metabolites had an adjusted *P*-value ≤ 0.05 and a mean bootstrapped VIP ≥ 1 in the PLS-DA model; of these, 109 metabolites were annotated (**Table 2**). The majority of cecal metabolites were markedly reduced in the HAMRS2 group compared to the low fiber group (Column "F" in **Supplemental Table 2A**). Three metabolites that were higher in the HAMRS2-fed rats were lactose, succinic acid and the resistant starch breakdown product maltose. The following cecal amino acids were significantly reduced in the HAMRS2 fed group: aspartic acid, isoleucine, leucine, lysine, methionine, phenylalanine, serine, and valine. Other nitrogenous metabolites that were significantly reduced in the HAMRS2 rats include: adenine, creatinine, indole-3-lactate, inosine, methionine sulfoxide, thymidine, uracil, urea, uric acid, uridine, and xanthine. The sugar alcohols 1,5-anhydroglucitol, galactinol, myo-inositol, and xylitol were also reduced in the HAMRS2-fed rats.

Serum Metabolites

A total of 300 serum metabolites were detected, 145 of which were annotated (**Supplemental Table S2B**). The abundances of 20 metabolites were found to be significantly different between treatment groups; 12 of which were annotated (**Table 3**). Two xeno-metabolites derived from microbial metabolism of tryptophan, indole-3-acetate and indole-3-lactate, were higher in the HAMRS2 fed rats. Two DNA bases, cytosine and thymidine, were reduced in the serum of HAMRS-fed rats. Another nitrogen-containing metabolite, uric acid, was reduced in the HAMRS2-fed rats compared to low fiber-fed rats. Two polyols, erythritol and xylitol, were greater in the HAMRS2 rats compared to low-fiber rats, respectively. Another polyol, 1,5-anhydroglucitol, was reduced in the HAMRS2-fed rats. The organic acids fumaric acid and malic acid were greater in the HAMRS2 fed rats. The ketone body β-hydroxybutyric acid was also greater in the HAMRS2-fed rats.

Urine Metabolites

In urine, 276 metabolites were detected and of these, 143 metabolites were annotated (**Supplemental Table S2C**). Abundances of 114 metabolites were significantly different between treatment groups; 47 of which were annotated (**Table 4**). There were 23 annotated metabolites for which concentrations were significantly increased in HAMRS2 rats. Tartaric acid was particularly noteworthy in the HAMRS2-fed rats; this metabolite had the highest VIP and greatest change of any urine metabolite. Three xeno-metabolites resulting from microbial metabolism were lower in the HAMRS2 group: 2,8-dihydroxyquinoline, 3-(3-hydroxyphenol)propionic acid, and 3-hydroxyphenolacetic acid. Concentrations of several amino acids were also higher in the HAMRS2 rat urine compared to the low fiber group: i.e., alanine, isoleucine, taurine, and tyrosine. The following sugars were higher in the HAMRS2 urine compared to the low fiber group: erythritol, fucose, inulotriose, maltose, ribose, sucrose, and xylitol. Several fatty acids were reduced in the HAMRS2 compared to the low fiber group:

capric, caprylic, heptadecanoic, myristic, and palmitic. The urine metabolomics dataset is also presented as estimated 24 hour excretion for each metabolite, in **Supplemental Table S2D.**

HAMRS2 alters uremic retention solutes

Trends in URS metabolite concentrations in the cecal contents, serum, and urine are compared in **Table 5**. Overall, most URS were reduced in cecal contents, with the exceptions of putrescine, erythritol and mannitol. Serum metabolite trends did not always track cecum concentration patterns, perhaps due to the dynamics of gut absorption coupled to kidney excretion—both of which would impact the net accumulation in the blood pool. For instance, cecal creatinine was 52% lower in the HAMRS2-fed rats, but this marked reduction was less apparent in serum. Urine creatinine concentration, on the other hand, was robustly increased. This may be due to improved creatinine clearance or reduced CKD-induced muscle wasting in the fiber fed rats. Notably, the metabolomics results for urinary creatinine were consistent with results from our previous report that utilized a more traditional enzyme-based creatinine assay (74); the values from the two types of analyses had a Spearman's correlation coefficient of 0.77 ($p<0.0001$). Urea was reduced by 79.0% in cecal contents, yet there was no change in serum; the latter is consistent with previous findings from these rats in which an enzyme-based urea assay was employed (74). Levels of uric acid were significantly lower in the serum and cecal contents, and ~50% higher in the urine of rats fed HAMRS2. HAMRS2-fed rats had 65.7% lower indoxyl sulfate in the urine and 36% lower abundance in the serum. Indoxyl sulfate was not reported as detectable in the cecal contents, consistent with the idea that the sulfate metabolite is produced by the host from microbe-derived indole (15). There were several other examples in which the various metabolite pools differed in the directionality of concentration between the treatment groups. For instance, there was no significant difference in urine and cecal indole-3-acetate between treatment groups, yet its serum level was 615% greater in the HAMRS2-fed rats. Indole-3-lactate abundance was reduced by ~70% in the cecal contents and

318 >50% in urine of HAMRS2-fed rats, yet its serum abundance was 135% higher compared to
319 low-fiber fed rats. *p*-cresol, derived from microbial transformation of tyrosine, was reduced by
320 47% in the urine of the HAMRS2 group, but was not reported as detectable in the serum or
321 cecal contents. Hippuric acid was reduced by >70% in the urine of HAMRS2 fed rats and not
322 reported as detectable in the serum or cecal contents. Erythritol concentration was greater in
323 serum and urine of the HAMRS2-fed rats, but was not different in cecal contents. Mannitol was
324 reduced in the serum but increased by >200% in the cecal contents of the HAMRS2-fed rats;
325 there was no change in urine abundance. No differences were observed in serum or urine
326 abundances of myo-inositol; however, cecal content abundance was reduced in the HAMRS2
327 group. Phenol was not reported as detectable in the serum, and was reduced by >70% in the
328 urine and cecal contents of the HAMRS2-fed rats.

329 Spearman's correlations between kidney function-relevant phenotype data, URS
330 metabolites and the cecal bacteria for all rats are depicted in **Figure 4**. Cecal bacteria were
331 included based on having greater than 0.05% mean relative abundance present in each group
332 and an adjusted p-value ≤ 0.05 when comparing microbiome differences between treatment
333 groups. Several bacteria groups were associated with improved kidney function as measured
334 by creatinine clearance, which co-varied with cecal changes reflective of HAMRS2 diet (i.e.,
335 cecal tissue weight, reduced pH, cecal hydration). These included, for instance, the
336 Bacteroidetes families S24-7 and Barnesiellaceae, the Firmicutes genus *Ruminococcus*, and
337 the Proteobacteria genus, *Sutterella*. The suite of bacteria that correlated with improved kidney
338 function also had negative correlations with cecal URS compounds such as creatinine, indole-3-
339 lactate, spermidine, urea, uric acid, phenol, and myo-inositol.

340

Discussion

Resistant starch may improve CKD outcomes by altering the gut environment and hence systemic exposure to certain metabolites or other gut-derived factors that may impinge upon inflammation and kidney function. Relevant to this concept, a microarray study of cecal tissue gene expression in healthy rats fed HAMRS2 revealed that genes involved in cell growth, proliferation, differentiation, mucin production, and tissue structure were differentially expressed compared to low fiber-fed rats (33); these changes may aid in reducing translocation of harmful substances into systemic circulation. In the current study, HAMRS2 increased cecal tissue growth and increased hydration of cecal contents. Resistant starch has been shown to increase fecal output in both humans and animal models (32, 49); increased fecal output may indicate decreased fecal transit time. A recent paper by Vandeputte et al. described how decreased fecal transit time and increased fecal hydration can alter the gut microbiota to favor the presence of rapidly-growing bacteria (71). Furthermore, increased loss of water—and accompanying electrolytes—through feces might help limit the systemic water load on the kidneys.

Significant reductions in several cecal content amino acids were observed which may be due to an increased need for nitrogen to maintain protein synthesis if bacteria are reproducing more rapidly (or, if there are more bacteria) and gut tissue growth is enhanced; thus, under HAMRS2-fed conditions the gut may be acting as a “nitrogen sink” (86). This would serve to sequester nitrogen in the gut, reducing the amount that enters portal circulation and hence lowering the nitrogen load on the liver and kidneys. A recent study found conventional mice had lower amino acids entering the hepatic portal vein compared to germfree mice. The authors attributed the lower level of amino acids to increased synthesis of microbial biomass (44).

Another interesting consideration is that HAMRS2 feeding might elicit increases in gut urea transporters; this would facilitate bacterial protein synthesis under conditions of resistant

starch feeding, considering the microbial conversion of urea to amino acid backbones. This could partially explain why resistant starch reduced blood urea in non-CKD animal models (32, 87). That said, in our CKD rats, metabolomics analysis revealed no diet-associated differences in serum urea. This may be due to reduced distal tubular urea reabsorption, which is a major component of the urine concentrating process and is disturbed in chronic interstitial nephropathy (25). It should be noted that HAMRS2, unlike many cereal fibers, is completely devoid of protein and therefore may be better suited at reducing the nitrogenous load on host liver and kidneys as well as reduce microbial fermentation of amino acids in the colon (4, 14).

To further explore relationships between metabolite abundances, cecal characteristics and specific microbe populations, a cross-correlation plot was created which revealed a variety of significant associations (**Figure 4**). This analysis is hypothesis-generating; i.e., one may ask if HAMRS2-driven reductions in cecal urea are the result of increasing urea utilization by microbes that display a negative correlation with urea concentration (*Allobaculum*, e.g.). Other possibilities for decreased cecal urea include trapping of urea and its degradation products by HAMRS2 or its HAMRS2 breakdown products, urea dilution in larger volume of the cecal content, or rapid elimination of urea occasioned by shortened fecal transit time. These events can simultaneously lower the detectable urea in cecal fluid and minimize enterohepatic recycling of urea. Increased amounts of urea and its breakdown products such as ammonia have been shown to increase gut permeability (9, 77). Ammonia is generated by the microbial metabolism of urea by the enzyme urease, which can be further converted to ammonium hydroxide. Ammonium hydroxide increases intestinal pH and can lead to disruption and loss of the intestinal tight junction proteins and thereby increase gut permeability (9, 78).

Recent study of the fecal microbiota in patients with end-stage renal disease has shown a marked expansion of bacteria that possess the urease enzyme, as well those expressing enzymes that ferment aromatic amino acids and produce indoles and *p*-cresol (84). Microbial

aromatic amino acid fermentation that results in the production of metabolites such as phenol, and microbial proteases that can act as virulence factors and target the host epithelium, are more active at a neutral or basic pH (43, 61, 62). Phenol, which was reduced in the cecal contents and urine of HAMRS2-fed rats, has been shown to have toxic effects on human colonic epithelial cells *in vitro* and contribute to increased intestinal permeability in CKD (36). The net effect of HAMRS2-associated cecal metabolite changes may be a reduction in the systemic exposure to potentially harmful URS metabolites in CKD such as the microbial-derived indole (converted to indoxyl sulfate by the host) and *p*-cresol. Metabolomics analysis revealed reductions in urinary levels of these URS metabolites and both were important in discriminating dietary treatment groups in PLS-DA models. Recently, it was shown that supplementing patients on hemodialysis with 15 grams per day of resistant starch for 6 weeks reduced plasma levels of unbound indoxyl sulfate (60), consistent with the results herein for CKD rats. It should be noted that indole itself may not be harmful and beneficial effects of indole and indole-3-acetate have been reported (5, 31). Some of the most robustly-increased serum metabolites in HAMRS2-fed CKD rats were indole-3-acetate and indole-3-lactate, despite unchanged or reduced levels in cecum and urine. The basis for this is not known, but it is speculated that resistant starch feeding increases microbial production of metabolites and/or effects changes to transporters or kidney reabsorption, which in turn drives relative accumulation in the blood pool. Another metabolite altered by HAMRS is uric acid. Uric acid and oxalic acid are normally excreted in the urine; however, in chronic renal failure the colon replaces the kidney as the primary site of their excretion (28, 29). This adaptive response may account for the minor rise in serum oxalic acid observed in HAMRS2-fed rats compared to the low fiber group (**Supplemental Table S2**).

Many other non-URS metabolites were also altered by HAMRS2 feeding. The metabolite with the greatest change was urinary tartaric acid, which was >800% greater in the

HAMRS2 group. Tartaric acid is generally associated with grape and wine consumption, so the etiology behind this striking increase remains to be elucidated. It likely involves HAMRS2-associated changes in gut microbe ecology and metabolism of chow components. Two other urinary metabolites that were significantly elevated in the HAMRS2 group were furoylglycine and levoglucosan. These metabolites have been reported to form due to heating foods at high temperatures and may have occurred during the manufacturing process of the rodent diets (10, 48). Increased levels in the urine may reflect enhanced urinary excretion in the HAMRS2 group due to improved kidney function. Other metabolites that have been reported to be modulated by the gut microbiota were also changed in the HAMRS2 group. Urinary hippuric acid was significantly reduced in the HAMRS2-fed rats. This metabolite can be formed in a few ways, one of which is by microbial metabolism of aromatic amino acids to form benzoic acid which the host can then conjugate with glycine to form hippuric acid (39, 82). Interestingly, the hippuric acid precursor benzoic acid was significantly reduced in the cecal contents and urine; there was no change in serum levels. Another microbial-derived metabolite, 3-(3-hydroxyphenyl)propionic acid (HPHPA), was reduced by ~85% in the urine and ~100% greater in the cecal contents of the HAMRS2-fed rats. Elevated urinary HPHPA levels have been found in individuals with autism and these levels decreased after antibiotic treatment, the latter speaking to the microbial origins of this xeno-metabolite (59). Several metabolites that have been reported to have antimicrobial activity were also changed in the HAMRS2 group including: 4-hydroxybenzoic acid, 3,4-dihydroxybenzoic acid, phenylacetic acid, 3-hydroxyphenylacetic acid, 4-hydroxyphenylacetic acid, and 3, 4-dihydroxyphenylacetic acid (13). In summary, changes in xeno-metabolites appear to reflect the dramatic shifts that occur in the gut microbiota with both HAMRS2 consumption and CKD.

The HAMRS2-fed rats exhibited less microbial diversity than the low fiber-fed rats. More microbial diversity is generally associated with a healthier phenotype (2). However, the

441 decrease in diversity observed in the HAMRS2 rats is likely due to the homogeneous
442 composition and configuration of HAMRS2. Decreased microbial diversity upon feeding
443 resistant starch has been previously reported (70). HAMRS2 is composed solely of glucose
444 with α-1,4 bonds (3). Fibers with a variety of monosaccharides and bond types likely select for
445 a more diverse microbial population simply by providing a wider array of substrates. A
446 significant increase in the Bacteroidetes:Firmicutes ratio was observed in the HAMRS2-fed rats.
447 A starch-related increase in the Bacteroidetes:Firmicutes ratio has been reported in previous
448 studies and has generally been associated with a healthy gut microbial community (67, 69).
449 Despite an overall reduction in Firmicutes, there was a bloom in the specific Firmicutes genera
450 *Ruminococcus. Ruminococcus bromii* has been described as a primary starch degrader that
451 provides substrates to other bacteria (89). We found that the relative abundance of
452 *Ruminococcus* and several other bacteria had negative correlations with cecal content pH. The
453 decrease in pH is likely due to increased microbial fermentation of the HAMRS2, resulting in
454 increased production of short-chain fatty acids such as acetate, propionate, and butyrate (7, 46).
455 A decreased intestinal pH is thought to be beneficial to the host by altering gut bacteria (i.e.
456 changes in metabolite production/utilization, growth, virulence factors) and maintaining the
457 integrity of the intestinal epithelium (57, 66). Another Firmicutes genera that was substantially
458 higher in the HAMRS2-fed rats was the butyrate-producer *Allobaculum*, which has been
459 associated with a lean phenotype and found to be increased in aged mice fed HAMRS2 (54,
460 67). However, *Allobaculum* has also been negatively correlated with colonic tight junction and
461 anti-inflammatory gene expression in the colon (37), making its putative role in host health less
462 certain.

463 The HAMRS2-fed group had an increase in the phylum Proteobacteria, with a bloom in
464 order RF32 (Alphaproteobacteria) and the genus *Sutterella* (Betaproteobacteria). There is
465 scant information related to *Sutterella*; this genus has been found to be elevated in the feces

and intestinal biopsies of children with autism (80, 81), and in feces from dogs with acute hemorrhagic diarrhea (65). We did observe decreased levels of the family Desulfovibrionaceae (Deltaproteobacteria) in the HAMRS2 rats. Bacteria from this family are capable of producing sulfide which may disrupt disulfide bridges in the protective mucus layer leading to increased intestinal permeability (38, 50). This bacteria has also been found to be increased in mice fed a high-fat diet and reduced by pre-biotic supplementation (18).

The intent of this study was to determine if HAMRS2-associated alterations in specific gut microbes as well as cecal, serum, and urine metabolites are correlated with one another and associate with the positive gut and renal outcomes previously reported for these rats (74); this has identified potential mechanisms by which resistant starch impacts kidney function and ameliorates CKD. To demonstrate this, the diet was supplemented 59% by weight with HAMRS2, which is a high amount relative to dietary supplementation in humans but is a level certain to elicit marked alterations in gut microbiota in this proof-of-principle experiment. Approximately 40% of the HAMRS2 is absorbed in the small intestine and the remaining portion reaches the colon where it can be degraded by microbes. Therefore, the amount of starch reaching the colon is approximately 36% by weight of the diet. Future experiments should be conducted to determine dose response, changes in gut permeability and if the phenotype can be replicated via cecal/fecal transplantation. A limitation of the current study that was not controlled for was coprophagy. Coprophagy may impact results from this, and other related rodent studies, by potentially influencing the recycling of microbes and metabolites. Therefore, extrapolation of these data—especially the serum and urine metabolites-- to the human condition may be limited. The impact of coprophagia on microbiota and metabolomics results warrants further investigation.

In summary, dietary resistant starch has a protective effect on kidney function in CKD rats that takes place concurrent with alterations in gut microbe ecology and shifts in specific

groupings of gut bacteria. Yet, the complete sets of mechanisms linking the microbiome and kidney function remain to be elucidated. Our results support the idea that resistant starch-associated phenotypes stem in part from change in the gut microbiome that alter URS dynamics, nitrogen and water balance, gut pH, and by minimizing inflammation via preservation of the gut epithelial barrier. A working model of the effects of HAMRS2 based on findings from this study and our previous results with the same rats is shown in **Figure 5**. Should the protective actions of HAMRS2 observed in the rat model recapitulate in human patients with developing or fulminant kidney disease, dietary resistant starch or other means to modify the microbiome could provide a new approach to complement existing medical therapies. Relevant in this regard, individuals consuming up to 45 grams HAMRS2 per day reported little to no gastrointestinal discomfort or gas (26), and HAMRS2 is inexpensive and readily incorporated into common foods such as yogurt, orange juice, and baked goods (22). Several epidemiological and clinical studies have shown that increased fiber intake can improve or delay the progression of CKD (35, 53, 88). Thus, HAMRS2 could provide a useful dietary adjunct to existing clinical strategies to retard CKD progression and its associated systemic inflammation and cardiovascular complications. Finally, our discussion of metabolites focused largely on URS and nitrogen-containing molecules. Yet, the survey of metabolism enabled by metabolomics analysis of cecal contents highlighted that modification of dietary resistant starch intake--and concomitant shifts in the gut microbiome--lead to dramatic alterations in gut lumen xeno-metabolite profiles. Elucidating how these metabolites contribute to the systemic metabolome, host health, intestinal function, and the gut microbial ecology presents an exciting frontier for research.

Source of support: The project was supported in part by a T32 training award (to DAK) funded by the National Center for Advancing Translational Sciences, National Institutes of Health,

through grant number UL1 TR000002 and linked award TL1 TR000133 and West Coast Comprehensive Metabolomics Center funded by the National Institutes of Health/NIDDK U24 DK097154. The content is solely the responsibility of the authors and does not necessarily represent the official views of the NIH. In addition, the authors wish to acknowledge funding support from Danish Council for Strategic Research, and USDA-ARS Projects 2032-51530-022-00D and 6026-51000-010-05S.

513

514

515 **Disclosures**

516 The authors have no conflict of interest. The authors acknowledge funding for this experiment.

517

References

1. K/DOQI clinical practice guidelines for bone metabolism and disease in chronic kidney disease. *American journal of kidney diseases : the official journal of the National Kidney Foundation* 42: S1-201, 2003.
2. Structure, function and diversity of the healthy human microbiome. *Nature* 486: 207-214, 2012.
3. **Annison G, and Topping DL**. Nutritional role of resistant starch: chemical structure vs physiological function. *Annual review of nutrition* 14: 297-320, 1994.
4. **Baker D**. Determing Fiber in Cereals. *Cereal Chemistry* 54: 360-365, 1977.
5. **Bansal T, Alaniz RC, Wood TK, and Jayaraman A**. The bacterial signal indole increases epithelial-cell tight-junction resistance and attenuates indicators of inflammation. *Proceedings of the National Academy of Sciences of the United States of America* 107: 228-233, 2010.
6. **Barreto FC, Barreto DV, Liabeuf S, Meert N, Glorieux G, Temmar M, Choukroun G, Vanholder R, and Massy ZA**. Serum indoxyl sulfate is associated with vascular disease and mortality in chronic kidney disease patients. *Clinical journal of the American Society of Nephrology : CJASN* 4: 1551-1558, 2009.
7. **Belobrajdic DP, King RA, Christophersen CT, and Bird AR**. Dietary resistant starch dose-dependently reduces adiposity in obesity-prone and obesity-resistant male rats. *Nutrition & Metabolism* 9: 93-93, 2012.
8. **Benjamini Y, and Hochberg Y**. Controlling the false discovery rate: a practical and powerful approach to multiple testing. *Journal of the Royal Statistical Society Series B (Methodological)* 289-300, 1995.
9. **Bourke E, Milne MD, and Stokes GS**. Caecal pH and ammonia in experimental uraemia. *Gut* 7: 558-561, 1966.
10. **Campbell C, Grapov D, Fiehn O, Chandler CJ, Burnett DJ, Souza EC, Casazza GA, Gustafson MB, Keim NL, and Newman JW**. Improved metabolic health alters host metabolism in parallel with changes in systemic xeno-metabolites of gut origin. *PloS one* 9: e84260, 2014.
11. **Caporaso JG, Kuczynski J, Stombaugh J, Bittinger K, Bushman FD, Costello EK, Fierer N, Pena AG, Goodrich JK, and Gordon JI**. QIIME allows analysis of high-throughput community sequencing data. *Nature methods* 7: 335-336, 2010.
12. **Caporaso JG, Lauber CL, Walters WA, Berg-Lyons D, Lozupone CA, Turnbaugh PJ, Fierer N, and Knight R**. Global patterns of 16S rRNA diversity at a depth of millions of sequences per sample. *Proc Natl Acad Sci U S A* 108 Suppl 1: 4516-4522, 2011.
13. **Cueva C, Moreno-Arribas MV, Martín-Álvarez PJ, Bills G, Vicente MF, Basilio A, Rivas CL, Requena T, Rodríguez JM, and Bartolomé B**. Antimicrobial activity of phenolic acids against commensal, probiotic and pathogenic bacteria. *Research in Microbiology* 161: 372-382, 2010.
14. **Cummings J, Hill M, Bone E, Branch W, and Jenkins D**. The effect of meat protein and dietary fiber on colonic function and metabolism. II. Bacterial metabolites in feces and urine. *The American journal of clinical nutrition* 32: 2094-2101, 1979.
15. **Cummings JH**. Fermentation in the human large intestine: evidence and implications for health. *Lancet (London, England)* 1: 1206-1209, 1983.
16. **De Schrijver R, Vanhoof K, and Vande Ginste J**. Nutrient utilization in rats and pigs fed enzyme resistant starch. *Nutrition Research* 19: 1349-1361.
17. **Earle Kristen A, Billings G, Sigal M, Lichtman Joshua S, Hansson Gunnar C, Elias Joshua E, Amieva Manuel R, Huang Kerwyn C, and Sonnenburg Justin L**. Quantitative Imaging of Gut Microbiota Spatial Organization. *Cell Host & Microbe* 18: 478-488.
18. **Everard A, Lazarevic V, Derrien M, Girard M, Muccioli GG, Neyrinck AM, Possemiers S, Van Holle A, François P, de Vos WM, Delzenne NM, Schrenzel J, and Cani PD**. Responses of Gut Microbiota

and Glucose and Lipid Metabolism to Prebiotics in Genetic Obese and Diet-Induced Leptin-Resistant Mice. *Diabetes* 60: 2775-2786, 2011.
19. **Fiehn O, and Kind T**. Metabolite profiling in blood plasma. *Methods in molecular biology (Clifton, NJ)* 358: 3-17, 2007.
20. **Fiehn O, Wohlgemuth G, and Scholz M**. Setup and Annotation of Metabolomic Experiments by Integrating Biological and Mass Spectrometric Metadata. In: *Data Integration in the Life Sciences*, edited by Ludäscher B, and Raschid LSpringer Berlin Heidelberg, 2005, p. 224-239.
21. **Flint HJ, Scott KP, Louis P, and Duncan SH**. The role of the gut microbiota in nutrition and health. *Nature reviews Gastroenterology & hepatology* 9: 577-589, 2012.
22. **Fuentes-Zaragoza E, Riquelme-Navarrete MJ, Sánchez-Zapata E, and Pérez-Álvarez JA**. Resistant starch as functional ingredient: A review. *Food Research International* 43: 931-942, 2010.
23. **Geurts L, Neyrinck AM, Delzenne NM, Knauf C, and Cani PD**. Gut microbiota controls adipose tissue expansion, gut barrier and glucose metabolism: novel insights into molecular targets and interventions using prebiotics. *Beneficial microbes* 5: 3-17, 2014.
24. **Gibson GR**. Dietary modulation of the human gut microflora using prebiotics. *The British journal of nutrition* 80: S209-212, 1998.
25. **Gilbert RM, Weber H, Turchin L, Fine LG, Bourgoignie JJ, and Bricker NS**. A study of the intrarenal recycling of urea in the rat with chronic experimental pyelonephritis. *Journal of Clinical Investigation* 58: 1348-1357, 1976.
26. **Grabitske HA, and Slavin JL**. Gastrointestinal Effects of Low-Digestible Carbohydrates. *Critical Reviews in Food Science and Nutrition* 49: 327-360, 2009.
27. **Hastie T, Tibshirani, R., Narasimhan, B., Chu, G.** impute: Imputation for microarray data.
28. **Hatch M, Freel RW, and Vaziri N**. Intestinal excretion of oxalate in chronic renal failure. *Journal of the American Society of Nephrology* 5: 1339-1343, 1994.
29. **Hatch M, and Vaziri N**. Enhanced enteric excretion of urate in rats with chronic renal failure. *Clinical Science* 86: 511-516, 1994.
30. **Jensen-Urstad AP, and Semenkovich CF**. Fatty acid synthase and liver triglyceride metabolism: housekeeper or messenger? *Biochim Biophys Acta* 1821: 747-753, 2012.
31. **Jin UH, Lee SO, Sridharan G, Lee K, Davidson LA, Jayaraman A, Chapkin RS, Alaniz R, and Safe S**. Microbiome-derived tryptophan metabolites and their aryl hydrocarbon receptor-dependent agonist and antagonist activities. *Molecular pharmacology* 85: 777-788, 2014.
32. **Kalmokoff M, Zwicker B, O'Hara M, Matias F, Green J, Shastri P, Green-Johnson J, and Brooks SP**. Temporal change in the gut community of rats fed high amylose cornstarch is driven by endogenous urea rather than strictly on carbohydrate availability. *Journal of applied microbiology* 114: 1516-1528, 2013.
33. **Keenan MJ, Martin RJ, Raggio AM, McCutcheon KL, Brown IL, Birkett A, Newman SS, Skaf J, Hegsted M, Tulley RT, Blair E, and Zhou J**. A microarray study indicates high-amylose resistant starch increases hormones and improves structure and function of the GI tract. *Journal of nutrigenetics and nutrigenomics* 5: 26-44, 2012.
34. **Komsta L**. outliers: Tests for outliers. 2011.
35. **Krishnamurthy VMR, Wei G, Baird BC, Murtaugh M, Chonchol MB, Raphael KL, Greene T, and Beddhu S**. High dietary fiber intake is associated with decreased inflammation and all-cause mortality in patients with chronic kidney disease. *Kidney international* 81: 300-306, 2012.
36. **Leclercq S, Matamoros S, Cani PD, Neyrinck AM, Jamar F, Stärkel P, Windey K, Tremaroli V, Bäckhed F, Verbeke K, de Timary P, and Delzenne NM**. Intestinal permeability, gut-bacterial dysbiosis, and behavioral markers of alcohol-dependence severity. *Proceedings of the National Academy of Sciences* 111: E4485-E4493, 2014.

37. **Lee SM, Han HW, and Yim SY**. Beneficial effects of soy milk and fiber on high cholesterol diet-induced alteration of gut microbiota and inflammatory gene expression in rats. *Food Funct* 6: 492-500, 2015.
38. **Lennon G, Balfe A, Bambury N, Lavelle A, Maguire A, Docherty NG, Coffey JC, Winter DC, Sheahan K, and O'Connell PR**. Correlations between colonic crypt mucin chemotype, inflammatory grade and Desulfovibrio species in ulcerative colitis. *Colorectal disease : the official journal of the Association of Coloproctology of Great Britain and Ireland* 16: O161-169, 2014.
39. **Lewis HB**. STUDIES IN THE SYNTHESIS OF HIPPURIC ACID IN THE ANIMAL ORGANISM II. THE SYNTHESIS AND RATE OF ELIMINATION OF HIPPURIC ACID AFTER BENZOATE INGESTION IN MAN. *Journal of Biological Chemistry* 18: 225-231, 1914.
40. **Li H, Ma M-L, Luo S, Zhang R-M, Han P, and Hu W**. Metabolic responses to ethanol in Saccharomyces cerevisiae using a gas chromatography tandem mass spectrometry-based metabolomics approach. *The international journal of biochemistry & cell biology* 44: 1087-1096, 2012.
41. **Lin CJ, Chuang CK, Jayakumar T, Liu HL, Pan CF, Wang TJ, Chen HH, and Wu CJ**. Serum p-cresyl sulfate predicts cardiovascular disease and mortality in elderly hemodialysis patients. *Archives of medical science : AMS* 9: 662-668, 2013.
42. **Lozupone C, and Knight R**. UniFrac: a New Phylogenetic Method for Comparing Microbial Communities. *Applied and Environmental Microbiology* 71: 8228-8235, 2005.
43. **Macfarlane GT, Allison C, Gibson SA, and Cummings JH**. Contribution of the microflora to proteolysis in the human large intestine. *The Journal of applied bacteriology* 64: 37-46, 1988.
44. **Mardinoglu A, Shoaie S, Bergentall M, Ghaffari P, Zhang C, Larsson E, Backhed F, and Nielsen J**. The gut microbiota modulates host amino acid and glutathione metabolism in mice. *Molecular systems biology* 11: 834, 2015.
45. **Mevik B, Wehrens, R., Liland, KH.** pls: Partial Least Squares and Principal Component regression. 2013.
46. **Morita T, Kasaoka S, Ohhashi A, Ikai M, Numasaki Y, and Kiriyama S**. Resistant proteins alter cecal short-chain fatty acid profiles in rats fed high amylose cornstarch. *J Nutr* 128: 1156-1164, 1998.
47. **Nasir O, Umbach AT, Rexhepaj R, Ackermann TF, Bhandaru M, Ebrahim A, Artunc F, Kempe DS, Puchchakayala G, Siraskar B, Foller M, Saeed A, and Lang F**. Effects of gum arabic (Acacia senegal) on renal function in diabetic mice. *Kidney & blood pressure research* 35: 365-372, 2012.
48. **Pettersen JE, and Jellum E**. The identification and metabolic origin of 2-furoylglycine and 2,5-furandicarboxylic acid in human urine. *Clinica Chimica Acta* 41: 199-207, 1972.
49. **Phillips J, Muir JG, Birkett A, Lu ZX, Jones GP, O'Dea K, and Young GP**. Effect of resistant starch on fecal bulk and fermentation-dependent events in humans. *The American journal of clinical nutrition* 62: 121-130, 1995.
50. **Pitcher MC, and Cummings JH**. Hydrogen sulphide: a bacterial toxin in ulcerative colitis? *Gut* 39: 1-4, 1996.
51. **R Core Team**. R: A Language and Environment for Statistical Computing,. Vienna, Austria: R Foundation for Statistical Computing, 2014.
52. **Ramezani A, and Raj DS**. The Gut Microbiome, Kidney Disease, and Targeted Interventions. *Journal of the American Society of Nephrology : JASN* 25: 657-670, 2014.
53. **Rampton D, Cohen S, Crammond V, Gibbons J, Lilburn M, Rabet J, Vince A, Wager J, and Wrong O**. Treatment of chronic renal failure with dietary fiber. *Clin Nephrol* 21: 159-163, 1984.
54. **Ravussin Y, Koren O, Spor A, LeDuc C, Gutman R, Stombaugh J, Knight R, Ley RE, and Leibel RL**. Responses of Gut Microbiota to Diet Composition and Weight Loss in Lean and Obese Mice. *Obesity (Silver Spring, Md)* 20: 10.1038/oby.2011.1111, 2012.
55. **Robert P**. Structural and Functional Adaptation in Renal Failure.—II. *Br Med J* 1: 1372-1377, 1952.

56. **Sanghavi S, Whiting S, and Uribarri J**. Potassium balance in dialysis patients. *Seminars in dialysis* 26: 597-603, 2013.
57. **Scheppach W**. Effects of short chain fatty acids on gut morphology and function. *Gut* 35: S35-S38, 1994.
58. **Scholz M, and Fiehn O**. SetupX--a public study design database for metabolomic projects. *Pacific Symposium on Biocomputing Pacific Symposium on Biocomputing* 169-180, 2007.
59. **Shaw W**. Increased urinary excretion of a 3-(3-hydroxyphenyl)-3-hydroxypropionic acid (HPHPA), an abnormal phenylalanine metabolite of Clostridia spp. in the gastrointestinal tract, in urine samples from patients with autism and schizophrenia. *Nutritional neuroscience* 13: 135-143, 2010.
60. **Sirich TL, Plummer NS, Gardner CD, Hostetter TH, and Meyer TW**. Effect of increasing dietary fiber on plasma levels of colon-derived solutes in hemodialysis patients. *Clinical journal of the American Society of Nephrology : CJASN* 9: 1603-1610, 2014.
61. **Smith EA, and Macfarlane GT**. Enumeration of human colonic bacteria producing phenolic and indolic compounds: effects of pH, carbohydrate availability and retention time on dissimilatory aromatic amino acid metabolism. *The Journal of applied bacteriology* 81: 288-302, 1996.
62. **Smith EA, and Macfarlane GT**. Formation of Phenolic and Indolic Compounds by Anaerobic Bacteria in the Human Large Intestine. *Microbial ecology* 33: 180-188, 1997.
63. **Sonnenburg Erica D, and Sonnenburg Justin L**. Starving our Microbial Self: The Deleterious Consequences of a Diet Deficient in Microbiota-Accessible Carbohydrates. *Cell Metabolism* 20: 779-786, 2014.
64. **Sonnenburg JL, Xu J, Leip DD, Chen C-H, Westover BP, Weatherford J, Buhler JD, and Gordon JI**. Glycan Foraging in Vivo by an Intestine-Adapted Bacterial Symbiont. *Science* 307: 1955-1959, 2005.
65. **Suchodolski JS, Markel ME, Garcia-Mazcorro JF, Unterer S, Heilmann RM, Dowd SE, Kachroo P, Ivanov I, Minamoto Y, Dillman EM, Steiner JM, Cook AK, and Toresson L**. The Fecal Microbiome in Dogs with Acute Diarrhea and Idiopathic Inflammatory Bowel Disease. *PloS one* 7: e51907, 2012.
66. **Sun Y, and O'Riordan MXD**. Regulation of Bacterial Pathogenesis by Intestinal Short-Chain Fatty Acids. *Advances in applied microbiology* 85: 93-118, 2013.
67. **Tachon S, Zhou J, Keenan M, Martin R, and Marco ML**. The intestinal microbiota in aged mice is modulated by dietary resistant starch and correlated with improvements in host responses. *FEMS Microbiol Ecol* 83: 299-309, 2013.
68. **Toyohara T, Akiyama Y, Suzuki T, Takeuchi Y, Mishima E, Tanemoto M, Momose A, Toki N, Sato H, Nakayama M, Hozawa A, Tsuji I, Ito S, Soga T, and Abe T**. Metabolomic profiling of uremic solutes in CKD patients. *Hypertens Res* 33: 944-952, 2010.
69. **Turnbaugh PJ, Ley RE, Mahowald MA, Magrini V, Mardis ER, and Gordon JI**. An obesity-associated gut microbiome with increased capacity for energy harvest. *Nature* 444: 1027-1131, 2006.
70. **Umu OC, Frank JA, Fangel JU, Oostindjer M, da Silva CS, Bolhuis EJ, Bosch G, Willats WG, Pope PB, and Diep DB**. Resistant starch diet induces change in the swine microbiome and a predominance of beneficial bacterial populations. *Microbiome* 3: 16, 2015.
71. **Vandeputte D, Falony G, Vieira-Silva S, Tito RY, Joossens M, and Raes J**. Stool consistency is strongly associated with gut microbiota richness and composition, enterotypes and bacterial growth rates. *Gut* 2015.
72. **Vanholder R, and De Smet R**. Pathophysiologic effects of uremic retention solutes. *Journal of the American Society of Nephrology : JASN* 10: 1815-1823, 1999.
73. **Vanholder R, Schepers E, Pletinck A, Nagler EV, and Glorieux G**. The uremic toxicity of indoxyl sulfate and p-cresyl sulfate: a systematic review. *Journal of the American Society of Nephrology : JASN* 25: 1897-1907, 2014.

74. **Vaziri ND, Liu SM, Lau WL, Khazaeli M, Nazertehrani S, Farzaneh SH, Kieffer DA, Adams SH, and Martin RJ**. High amylose resistant starch diet ameliorates oxidative stress, inflammation, and progression of chronic kidney disease. *PloS one* 9: e114881, 2014.
75. **Vaziri ND, Wong J, Pahl M, Piceno YM, Yuan J, DeSantis TZ, Ni Z, Nguyen T-H, and Andersen GL**. Chronic kidney disease alters intestinal microbial flora. *Kidney international* 83: 308-315, 2013.
76. **Vaziri ND, Wong J, Pahl M, Piceno YM, Yuan J, DeSantis TZ, Ni Z, Nguyen TH, and Andersen GL**. Chronic kidney disease alters intestinal microbial flora. *Kidney international* 83: 308-315, 2013.
77. **Vaziri ND, Yuan J, and Norris K**. Role of urea in intestinal barrier dysfunction and disruption of epithelial tight junction in CKD. *American journal of nephrology* 37: 1-6, 2013.
78. **Vaziri ND, Yuan J, Rahimi A, Ni Z, Said H, and Subramanian VS**. Disintegration of colonic epithelial tight junction in uremia: a likely cause of CKD-associated inflammation. *Nephrology, dialysis, transplantation : official publication of the European Dialysis and Transplant Association - European Renal Association* 27: 2686-2693, 2012.
79. **Wang F, Jiang H, Shi K, Ren Y, Zhang P, and Cheng S**. Gut bacterial translocation is associated with microinflammation in end-stage renal disease patients. *Nephrology (Carlton, Vic)* 17: 733-738, 2012.
80. **Wang L, Christophersen C, Sorich M, Gerber J, Angley M, and Conlon M**. Increased abundance of Sutterella spp. and Ruminococcus torques in feces of children with autism spectrum disorder. *Molecular Autism* 4: 42, 2013.
81. **Williams BL, Hornig M, Parekh T, and Lipkin WI**. Application of novel PCR-based methods for detection, quantitation, and phylogenetic characterization of Sutterella species in intestinal biopsy samples from children with autism and gastrointestinal disturbances. *mBio* 3: 2012.
82. **Williams RE, Eyton-Jones HW, Farnworth MJ, Gallagher R, and Provan WM**. Effect of intestinal microflora on the urinary metabolic profile of rats: a (1)H-nuclear magnetic resonance spectroscopy study. *Xenobiotica; the fate of foreign compounds in biological systems* 32: 783-794, 2002.
83. **Wold S, Sjöström M, and Eriksson L**. PLS-regression: a basic tool of chemometrics. *Chemometrics and intelligent laboratory systems* 58: 109-130, 2001.
84. **Wong J, Piceno YM, Desantis TZ, Pahl M, Andersen GL, and Vaziri ND**. Expansion of urease- and uricase-containing, indole- and p-cresol-forming and contraction of short-chain fatty acid-producing intestinal microbiota in ESRD. *American journal of nephrology* 39: 230-237, 2014.
85. **Wong J, Piceno YM, DeSantis TZ, Pahl M, Andersen GL, and Vaziri ND**. Expansion of urease-and uricase-containing, indole-and p-cresol-forming and contraction of short-chain fatty acid-producing intestinal microbiota in ESRD. *American journal of nephrology* 39: 230-237, 2014.
86. **Younes H, Alphonse J-C, Behr SR, Demigné C, and Rémésy C**. Role of fermentable carbohydrate supplements with a low-protein diet in the course of chronic renal failure: Experimental bases. *American Journal of Kidney Diseases* 33: 633-646, 1999.
87. **Younes H, Demigné C, Behr S, and Rémésy C**. Resistant starch exerts a lowering effect on plasma urea by enhancing urea N transfer into the large intestine. *Nutrition Research* 15: 1199-1210, 1995.
88. **Younes H, Egret N, Hadj-Abdelkader M, Rémésy C, Demigné C, Gueret C, Deteix P, and Alphonse J-C**. Fermentable Carbohydrate Supplementation Alters Nitrogen Excretion in Chronic Renal Failure. *Journal of Renal Nutrition* 16: 67-74, 2006.
89. **Ze X, Duncan SH, Louis P, and Flint HJ**. Ruminococcus bromii is a keystone species for the degradation of resistant starch in the human colon. *Isme j* 6: 1535-1543, 2012.

Titles and Legends

TABLE 1. Cecal characteristics and bacterial phyla distribution in male CKD rats fed a low fiber diet or HAMRS2.

TABLE 2. Cecal annotated metabolites with mean bootstrapped VIP ≥1 in PLS-DA models, and a false discovery rate MWU p-value ≤ 0.05, ranked by percent change in HAMRS2-fed CKD rats relative to low fiber fed CKD controls.

TABLE 3. Serum annotated metabolites with mean bootstrapped VIP ≥1 in PLS-DA models, and a false discovery rate MWU p-value ≤ 0.05, ranked by percent change in HAMRS2-fed CKD rats relative to low fiber fed CKD controls.

TABLE 4. Urine annotated metabolites with mean bootstrapped VIP ≥1 in PLS-DA models, and a false discovery rate MWU p-value ≤ 0.05, ranked by percent change in HAMRS2-fed CKD rats relative to low fiber fed CKD controls.

TABLE 5. Percent changes in uremic retention solutes in cecal contents, serum , and urine in male CKD rats fed HAMRS2, relative to low fiber-fed CKD controls.

TABLE 6. General patterns of metabolite changes in cecal contents, serum, and urine in male CKD rats fed HAMRS2, relative to low fiber-fed CKD controls.

Supplemental TABLE S1. Cecal Bacteria Taxon Percent Abundances in male CKD rats fed a low fiber diet or HAMRS2.

Supplemental TABLES S2A-D. Cecal, serum, urine and 24 hour urine metabolites in male CKD rats fed a low fiber diet or HAMRS2. n=9/group.

FIGURE 1. Principal Coordinates Analysis scores plots of cecal contents, serum, and urine metabolites from male CKD rats in the model validation group fed a low fiber diet or HAMRS2. Ellipses represent 95% confidence intervals based on Hotelling's T2 statistic and each symbol represents a rat. Metabolites that contributed to these plots can be found in Tables 2-4.

Metabolomics was performed on 9 rats per group, model developed using 6 rats per group and model validation was performed using 3 rats per group.

FIGURE 2A. Unweighted UniFrac Beta-Diversity Principal Coordinates Analysis plot displays separation between treatment groups based on the cecal microbiota of male CKD rats fed a low fiber diet or HAMRS2. Axes represent percent of the variance that can be accounted for based on cecal microbiota profile. Ellipses represent 95% confidence intervals based on Hotelling's T2 statistic and each symbol represents a rat. n=9/group.

FIGURE 2B. Percent change of select cecal bacteria in CKD-HAMRS2 rats relative to the CKD-Low Fiber group. Bacteria included had a minimum of 0.05% mean abundance in each group and p-value ≤0.05. Bacteria are listed to the lowest level of classification (i.e. if last taxon assignment is f_, family is the lowest level of classification. p_=phylum, o_=order, f_=family, g_=genus). n=9/group

FIGURE 3. Partial Least Squares-Discriminant Analysis scores plots based on serum, urine, and cecal metabolites of male CKD rats fed a low fiber diet or HAMRS2. Ellipses represent 95% confidence intervals based on Hotelling's T2 statistic and each symbol represents a rat. Metabolites that contributed to these plots can be found in Tables 2-4. Metabolomics was performed on 9 rats per group, model developed using 6 rats per group and model validation was performed using 3 rats per group. QIPH: Quantifier Ion Peak Heights

FIGURE 4. Spearman's correlation matrix of cecal bacteria versus meta-data and uremic retention solutes in cecal contents, serum, and urine of male CKD rats fed a low fiber diet or HAMRS2 . Bacteria included had a minimum of 0.05% mean abundance in each group and an adjusted Mann-Whitney U p-value ≤0.05. Bacteria are listed to the lowest level of classification (i.e. if last taxon assignment is f_, family is the lowest level of classification. p_=phylum, o_=order, f_=family, g_=genus). Metabolites were selected based on being identified as URS. Those metabolites that had a mean bootstrapped VIP≥1 are indicated with an asterisk (*). Colonic tight junction data was imputed for two rats per group using k-nearest neighbors as described in the materials and methods. Direction of ellipses represent positive or negative correlation and width of ellipse represents strength of correlation (narrow ellipse=stronger correlation).

FIGURE 5. Working model of how HAMRS2 may improve CKD.

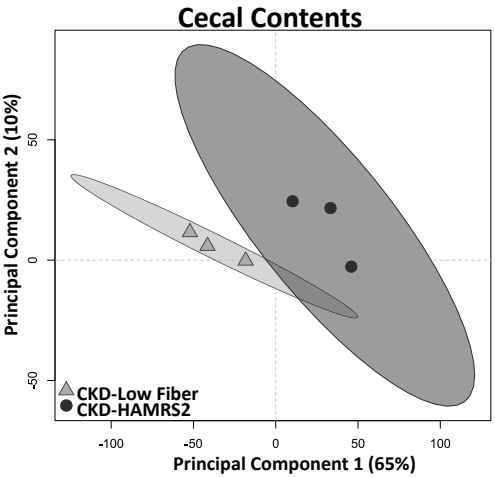
Cecal Contents
Principal Component 2 (10%)
Principal Component 1 (65%)
CKD-Low Fiber
CKD-HAMRS2

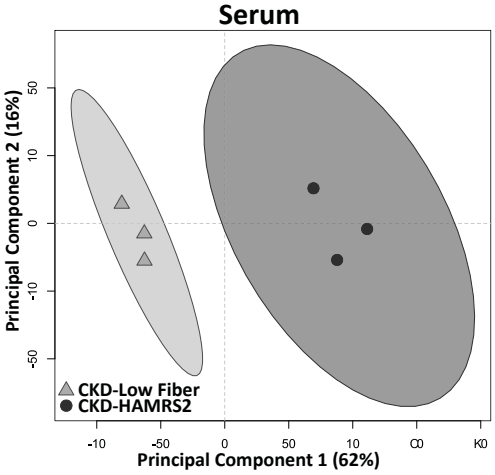
Serum
Principal Component 2 (16%)
Principal Component 1 (62%)
CKD-Low Fiber
CKD-HAMRS2

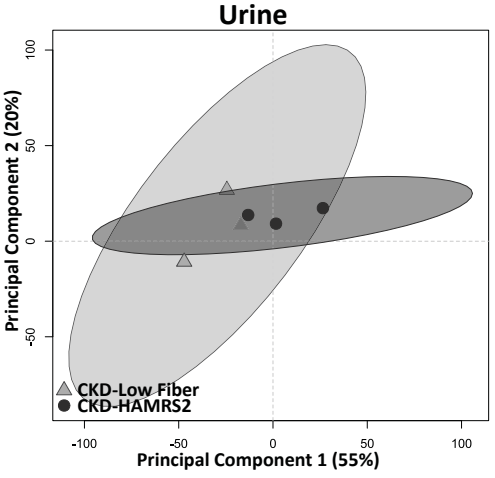
Urine
Principal Component 2 (20%)
Principal Component 1 (55%)
CKD-Low Fiber
CKD-HAMRS2

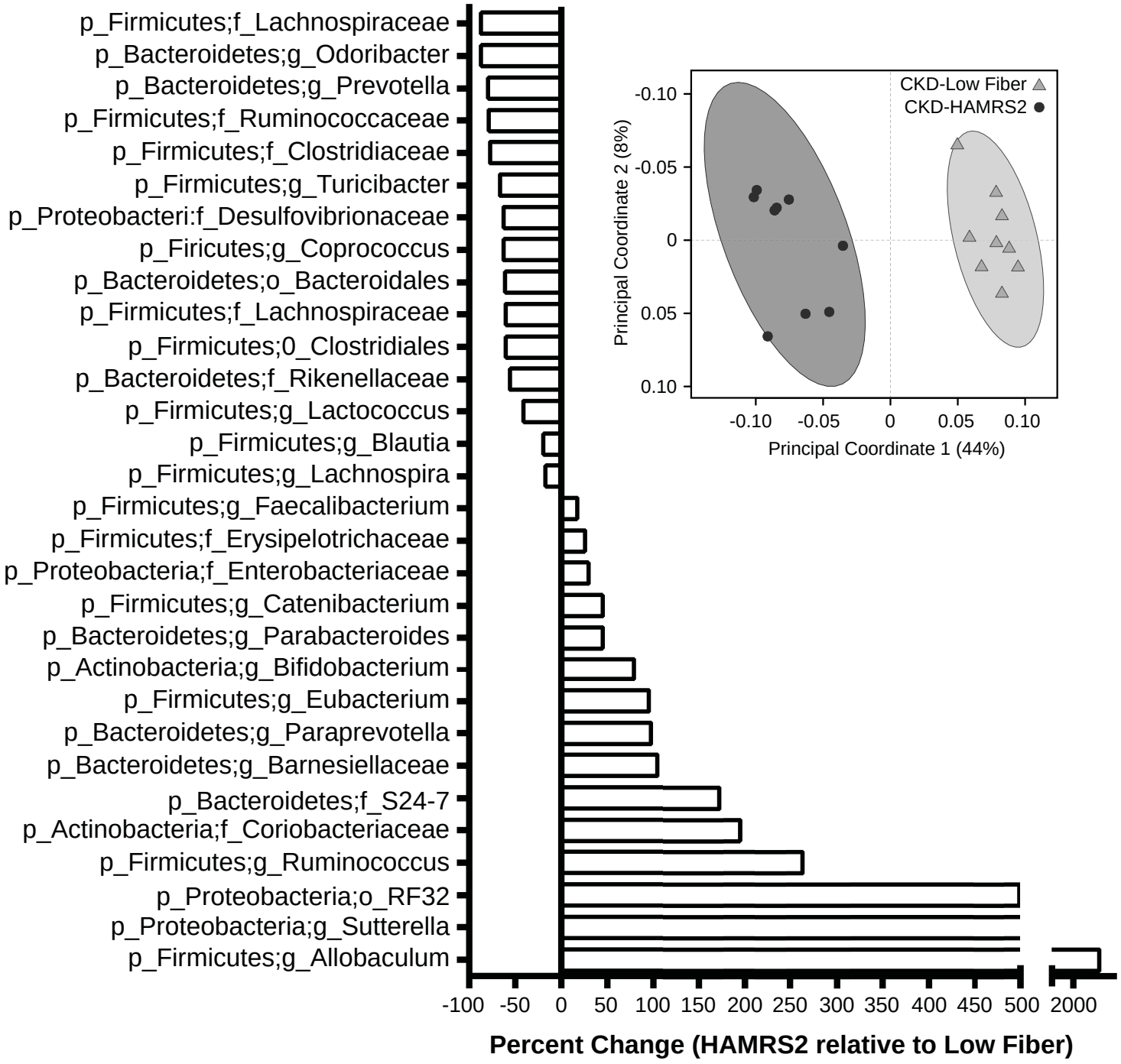
p_Firmicutes;f_Lachnospiraceae
p_Bacteroidetes;g_Odoribacter
p_Bacteroidetes;g_Prevotella
p_Firmicutes;f_Ruminococcaceae
p_Firmicutes;f_Clostridiaceae
p_Firmicutes;g_Turicibacter
p_Proteobacteri:f_Desulfovibrionaceae
p_Firicutes;g_Coprococcus
p_Bacteroidetes;o_Bacteroidales
p_Firmicutes;f_Lachnospiraceae
p_Firmicutes;0_Clostridiales
p_Bacteroidetes;f_Rikenellaceae
p_Firmicutes;g_Lactococcus
p_Firmicutes;g_Blautia
p_Firmicutes;g_Lachnospira
p_Firmicutes;g_Faecalibacterium
p_Firmicutes;f_Erysipelotrichaceae
p_Proteobacteria;f_Enterobacteriaceae
p_Firmicutes;g_Catenibacterium
p_Bacteroidetes;g_Parabacteroides
p_Actinobacteria;g_Bifidobacterium
p_Firmicutes;g_Eubacterium
p_Bacteroidetes;g_Paraprevotella
p_Bacteroidetes;g_Barnesiellaceae
p_Bacteroidetes;f_S24-7
p_Actinobacteria;f_Coriobacteriaceae
p_Firmicutes;g_Ruminococcus
p_Proteobacteria;o_RF32
p_Proteobacteria;g_Sutterella
p_Firmicutes;g_Allobaculum
-100 -50 0 50 100 150 200 250 300 350 400 450 500 2000
Percent Change (HAMRS2 relative to Low Fiber)
CKD-Low Fiber
CKD-HAMRS2
Principal Coordinate 2 (8%)
-0.10 -0.05 0 0.05 0.10
Principal Coordinate 1 (44%)
-0.10 -0.05 0 0.05 0.10

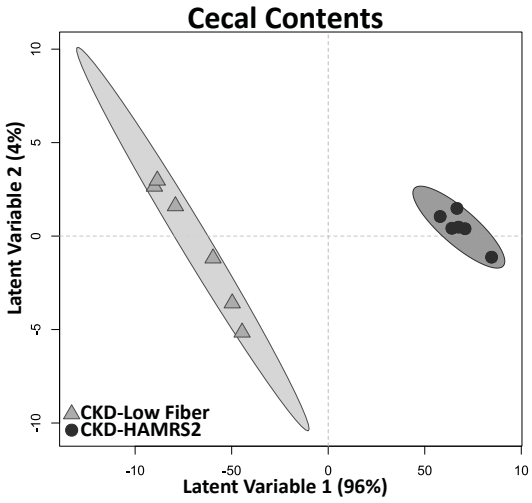
Cecal Contents
Latent Variable 2 (4%)
Latent Variable 1 (96%)
CKD-Low Fiber
CKD-HAMRS2

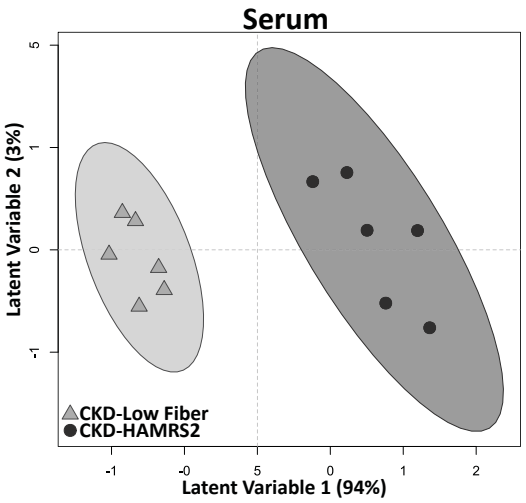
Serum
Latent Variable 2 (3%)
Latent Variable 1 (94%)
CKD-Low Fiber
CKD-HAMRS2

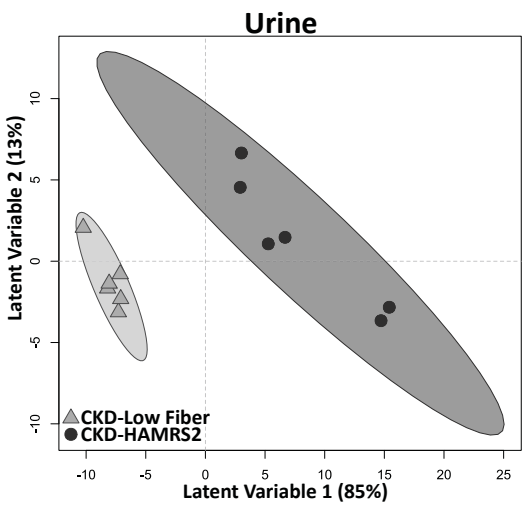
Urine
Latent Variable 2 (13%)
Latent Variable 1 (85%)
CKD-Low Fiber
CKD-HAMRS2

Metabolite Class
Nitrogenous
Polyol
Phenol
p_Actinobacteria;g_Bifidobacterium
p_Actinobacteria;f_Coriobacteriaceae
p_Bacteroidetes;g_Parabacteroides
p_Bacteroidetes;f_S24-7
p_Bacteroidetes;f_Barnesiellaceae
p_Bacteroidetes;g_Paraprevotella
p_Firmicutes;g_Faecalibacterium
p_Firmicutes;g_Ruminococcus
p_Firmicutes;f_Erysipelotrichaceae
p_Firmicutes;g_Allobaculum
p_Firmicutes;g_Catenibacterium
p_Firmicutes;g_Eubacterium
p_Proteobacteria;o_RF32
p_Proteobacteria;g_Sutterella
p_Proteobacteria;f_Enterobacteriaceae
p_Bacteroidetes;o_Bacteroidales
p_Bacteroidetes;f_Rikenellaceae
p_Bacteroidetes;g_Odoribacter
p_Bacteroidetes;g_Prevotella
p_Firmicutes;g_Lactococcus
p_Firmicutes;g_Turicibacter
p_Firmicutes;o_Clostridiales
p_Firmicutes;f_Clostridiaceae
p_Firmicutes;f_Lachnospiraceae
p_Firmicutes;g_Blautia
p_Firmicutes;g_Coprococcus
p_Firmicutes;g_Lachnospira
p_Firmicutes;f_Lachnospiraceae
p_Firmicutes;f_Ruminococcaceae
p_Proteobacteria;f_Desulfovibrionaceae
creatinine clearance
cecal dry matter
cecal tissue weight
cecal pH
colon claudin-1
colon occludin
cecal content
*creatinine
indole-3-acetate
*indole-3-lactate
putrescine
spermidine
*urea
*uric acid
erythritol
*mannitol
*myo-inositol
*phenol
serum
creatinine
*indole-3-acetate
*indole-3-lactate
indoxyl sulfate
urea
*uric acid
*erythritol
*mannitol
myo-inositol
urine
creatinine
*hippuric acid
indole-3-acetate
*indole-3-lactate
*indoxyl sulfate
*p-cresol
*putrescine
*spermidine
*urea
uric acid
erythritol
*mannitol
myo-inositol
*phenol
Spearman's Correlation Coefficient
-1
-0.8
-0.6
-0.4
-0.2
0
0.2
0.4
0.6
0.8
1

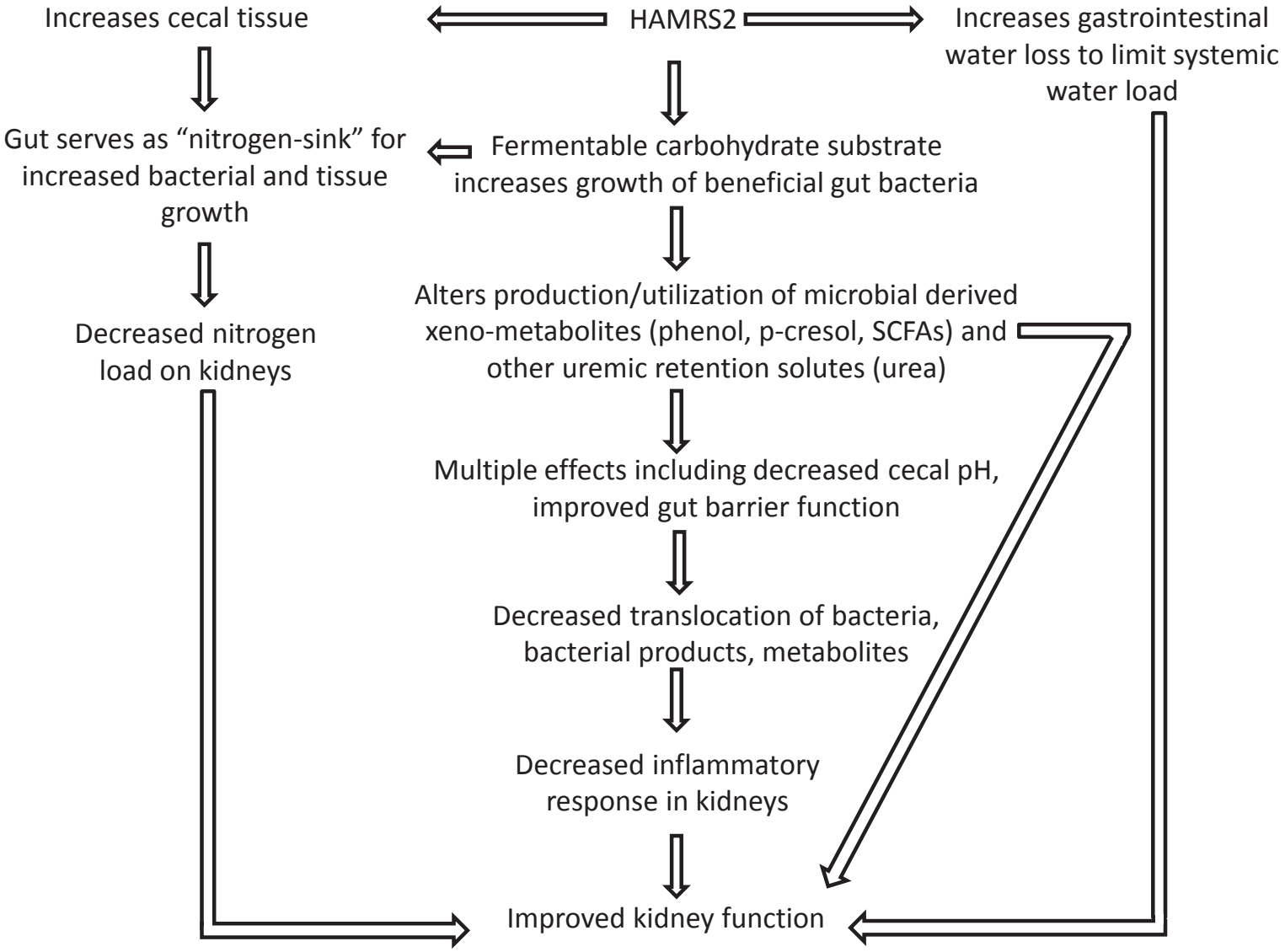
Increases cecal tissue
HAMRS2
Increases gastrointestinal water loss to limit systemic water load
Gut serves as “nitrogen-sink” for increased bacterial and tissue growth
Fermentable carbohydrate substrate increases growth of beneficial gut bacteria
Decreased nitrogen load on kidneys
Alters production/utilization of microbial derived xeno-metabolites (phenol, p-cresol, SCFAs) and other uremic retention solutes (urea)
Multiple effects including decreased cecal pH, improved gut barrier function
Decreased translocation of bacteria, bacterial products, metabolites
Decreased inflammatory response in kidneys
Improved kidney function

TABLE 1. Cecal characteristics and bacterial phyla distribution in male CKD rats fed a low fiber diet or HAMRS2[1].

Variable	CKD-Low Fiber	CKD-HAMRS2	p-value
Percent dry matter of cecal contents	23.1% ± 0.75	19.7% ± 0.95	0.011
Cecal weight (g)	0.7343 ± 0.053	1.937 ± 0.098	<0.0001
Cecal pH	8.09 ± 0.05	6.75 ± 0.16	<0.0001
Number of observed microbial species in cecum	791 ± 4	673 ± 12	<0.0001
Phylum	CKD-Low Fiber	CKD-HAMRS2	FDR p-value
Unassigned	0.43% ± 0.06	0.66% ± 0.35	0.6261
Actinobacteria	0.73% ± 0.05	1.34% ± 0.18	0.0086
Bacteroidetes	19.36% ± 2.82	27.49% ± 1.98	0.1094
Firmicutes	77.32% ± 2.72	64.77% ± 2.58	0.0181
Proteobacteria	1.51% ± 0.07	4.73% ± 0.61	0.0027
Tenericutes	0.58% ± 0.16	0.98% ± 0.65	0.6831
Verrumicrobia	0.07% ± 0.04	0.04% ± 0.004	0.6831
Bacteroidetes:Firmicutes ratio	0.26 ± 0.05	0.44 ± 0.05	0.02

[1]Values are means ± SEM; n=9 per group; FDR, false discovery rate

TABLE 2: Cecal metabolite characteristics of male rats with chronic kidney disease fed a low-fiber or HAMRS2 supplemented diet.[1]

Cecal Contents

Metabolite	CKD-Low Fiber Mean ± SEM	CKD-HAMRS2 Mean ± SEM	Percent Change	*P*[2]	VIP[3]
Amino Acids					
serine	43444.3 ± 2742.1	33057.7 ± 6846.4	-24%	0.02	1.16
valine	225602.4 ± 12889.2	152212.7 ± 33535.6	-33%	0.02	1.09
lysine	149830.3 ± 19852.5	100913 ± 27205.2	-33%	0.02	1.01
methionine	23834.4 ± 2557.4	12149.7 ± 3021.5	-49%	0.012	1.14
aspartic acid	264657.2 ± 48166.6	128401.8 ± 27873.9	-51%	0.012	1.04
isoleucine	111782.2 ± 9227.6	49476.5 ± 8454.1	-56%	<0.0001	1.19
phenylalanine	50456.3 ± 5242.2	20266.7 ± 5402.5	-60%	0.002	1.00
leucine	206390.4 ± 21887	46656.4 ± 11976.8	-77%	<0.0001	1.15
Other Nitrogenous Metabolites					
glycyl proline	4677.5 ± 444	3800.3 ± 2659.7	-19%	0.01	1.26
oxoproline	241076.5 ± 27920.3	114907.7 ± 16551.6	-52%	0.002	1.08
creatinine	2290.5 ± 363.9	1087.2 ± 228.4	-53%	0.007	1.08
trans-4-hydroxy-L-proline	2060.6 ± 368	855.7 ± 122.6	-58%	0.002	1.01
methionine sulfoxide	13339.5 ± 1135.3	5522.4 ± 686.9	-59%	<0.0001	1.23
maleimide	3121.1 ± 220.5	1167.6 ± 153.6	-63%	<0.0001	1.26
adenosine-5-monophosphate	2765.8 ± 414.1	1011.3 ± 309.9	-63%	0.002	1.09
ethanolamine	31963.1 ± 4555.3	11460.5 ± 1778.1	-64%	0.002	1.12
pyrrole-2-carboxylic acid	2322.4 ± 265.7	823.5 ± 63.4	-65%	<0.0001	1.11
N-acetyl-D-hexosamine	7645.4 ± 717.3	2535.4 ± 557.8	-67%	<0.0001	1.18
N-acetylglutamate	2451.4 ± 492.3	807.3 ± 266.3	-67%	0.005	1.06
5-deoxy-5-methylthioadenosine	2646.7 ± 361.5	843.5 ± 88.5	-68%	<0.0001	1.19
nicotinic acid	48218.4 ± 5940.8	15342.4 ± 3685.3	-68%	<0.0001	1.03
phosphoethanolamine	1148.8 ± 147.8	362.9 ± 77.6	-68%	0.002	1.11
hydroxycarbamate	1743.1 ± 161.5	529 ± 78.7	-70%	<0.0001	1.21
4-pyridoxic acid	1281.1 ± 261	387.9 ± 58.4	-70%	<0.0001	1.11
5-methoxytryptamine	13583 ± 1989.7	3921.6 ± 552	-71%	<0.0001	1.12
indole-3-lactate	5236.1 ± 768.7	1482.7 ± 408.7	-72%	<0.0001	1.05
epsilon caprolactam	7419.9 ± 836.4	1919.6 ± 267.9	-74%	<0.0001	1.22
UDP-N-acetylglucosamine	1528.6 ± 459.7	395.2 ± 86.1	-74%	0.002	1.08
hydroxylamine	11307 ± 1514.3	2871 ± 352	-75%	<0.0001	1.19
urea	6541.4 ± 795.6	1373.9 ± 138	-79%	<0.0001	1.21
uracil	45220.5 ± 4289.8	8969.8 ± 1785.4	-80%	<0.0001	1.19
xanthine	10992.1 ± 1241.4	2177.1 ± 461.3	-80%	<0.0001	1.17

N-acetylgalactosamine	12823 ± 1604.4	2448.7 ± 420.7	-81%	<0.0001	1.22
5-hydroxy-3-indoleacetic acid	3188.8 ± 672.8	538.7 ± 49.5	-83%	<0.0001	1.19
uridine	14453.6 ± 2591.4	2220.9 ± 785.9	-85%	<0.0001	1.19
N-acetylmannosamine	3326.3 ± 1196.1	508.8 ± 79.3	-85%	<0.0001	1.16
uric acid	2105.1 ± 310.4	313.2 ± 70.2	-85%	<0.0001	1.22
pseudo-uridine	5208.8 ± 844.3	754.2 ± 204.9	-86%	<0.0001	1.15
thymidine	5173.3 ± 955.2	705.7 ± 309.7	-86%	<0.0001	1.22
N-acetylaspartic acid	14061.1 ± 1755.9	1590.1 ± 350.6	-89%	<0.0001	1.23
inosine	46887 ± 10785.8	3185.4 ± 1122.9	-93%	<0.0001	1.13
Lipids					
nonadecanoic acid	3610.6 ± 358.3	1626.2 ± 169.3	-55%	0.002	1.13
cholesterol	39072.7 ± 3735.8	14822.3 ± 2475.1	-62%	<0.0001	1.06
myristic acid	32541.3 ± 4157.9	11530.2 ± 1072.1	-65%	<0.0001	1.21
heptadecanoic acid	26909.5 ± 3680.6	9442 ± 869.3	-65%	<0.0001	1.20
beta sitosterol	110165 ± 15754.3	38054.2 ± 3766.6	-65%	<0.0001	1.09
octadecanol	5076 ± 703.4	1745.5 ± 486	-66%	0.005	1.09
isoheptadecanoic acid	16336 ± 1949	4922 ± 1491.5	-70%	0.002	1.21
capric acid	1806.5 ± 195.4	515.8 ± 83.9	-71%	<0.0001	1.24
stearic acid	1196670.9 ± 174737.5	340323.5 ± 23564.8	-72%	<0.0001	1.25
cerotinic acid	2312.2 ± 368.4	643.1 ± 75.6	-72%	<0.0001	1.16
palmitic acid	167954.1 ± 27149	46428 ± 3412.1	-72%	<0.0001	1.23
2,4-hexadienedioic acid	1316.5 ± 169.4	322.3 ± 53.8	-76%	<0.0001	1.22
arachidic acid	60200.6 ± 10426.6	14142.7 ± 1374.3	-77%	<0.0001	1.18
cholestan-3-ol	24019.1 ± 3967.6	5422.7 ± 539	-77%	<0.0001	1.15
linoleic acid	13161 ± 3851.3	2791.5 ± 543.5	-79%	0.002	1.01
stigmasterol	11333.5 ± 1508	2304.3 ± 219.8	-80%	<0.0001	1.20
lauric acid	20617.6 ± 2496.1	3380.4 ± 635.3	-84%	<0.0001	1.22
phytol	3508.9 ± 539.8	479.7 ± 71.1	-86%	<0.0001	1.15
Carbohydrates					
maltose	564929.4 ± 86191.8	3231747.1 ± 192336.	472%	<0.0001	1.20
lactose	12348.6 ± 3868.6	60782.5 ± 11649.2	392%	<0.0001	1.00
ribose	161964.7 ± 22717.2	60156.3 ± 11073.9	-63%	<0.0001	1.01
6-deoxyglucose	35299.7 ± 4108.1	11454.5 ± 3485.9	-68%	0.002	1.06
3,6-anhydro-D-galactose	3058.4 ± 441.9	983.5 ± 65.7	-68%	<0.0001	1.08
1,5-anhydroglucitol	2702.2 ± 416	732.8 ± 79.6	-73%	<0.0001	1.19
xylitol	2318.3 ± 223.2	610.1 ± 133.5	-74%	<0.0001	1.07
xylulose	8667.4 ± 959.9	2206.6 ± 397.3	-75%	<0.0001	1.16
pinitol	1042.6 ± 159.5	239.3 ± 25.4	-77%	<0.0001	1.14
threonic acid	2039.1 ± 366.8	443.7 ± 81	-78%	<0.0001	1.09
myo-inositol	12685.8 ± 2773.1	2123.8 ± 379.7	-83%	<0.0001	1.14
fucose	111501.7 ± 15245.8	18341.1 ± 3357.4	-84%	<0.0001	1.20
galactinol	9455.7 ± 1485.3	746 ± 199.5	-92%	<0.0001	1.20
lyxose	56930.9 ± 14883.6	1328.6 ± 335.8	-98%	<0.0001	1.22

xylose	504305.2 ± 67733.7	4899.4 ± 596.5	-99%	<0.0001	1.28
Other Metabolites					
succinic acid	502829.7 ± 462586.3	2659290.5 ± 226139.	429%	0.005	1.27
lactic acid	66885 ± 7178.2	39474.2 ± 17482.1	-41%	0.007	1.13
2-hydroxybutanoic acid	6727.5 ± 640	2915.1 ± 1076	-57%	0.01	1.26
dihydroxyacetone	6276.1 ± 820.4	1986.4 ± 530.2	-68%	0.002	1.13
propane-1,3-diol	54707.3 ± 4623.7	17201.4 ± 1686.8	-69%	<0.0001	1.25
glyceric acid	52044.2 ± 6060.3	16186.2 ± 6607.7	-69%	0.007	1.16
adipic acid	3097.4 ± 446.4	958.6 ± 124.7	-69%	<0.0001	1.12
ribonic acid	1165.3 ± 132.6	350.9 ± 44.7	-70%	<0.0001	1.21
3-hydroxyphenylacetic acid	3661.5 ± 608.4	1077.4 ± 111	-71%	<0.0001	1.02
glycerol alpha phosphate	5536.2 ± 764.1	1494.4 ± 156.2	-73%	<0.0001	1.20
glycerol-3-galactoside	1888.2 ± 210.5	505.5 ± 32.2	-73%	<0.0001	1.24
dehydroabietic acid	2119 ± 252.6	549.9 ± 52.5	-74%	<0.0001	1.18
phenol	5565 ± 846.1	1441.9 ± 124.1	-74%	<0.0001	1.17
shikimic acid	6306.6 ± 654.7	1535.5 ± 296.1	-76%	<0.0001	1.22
gamma tocopherol	18386.5 ± 3081.9	4197.8 ± 196.9	-77%	<0.0001	1.18
hexuronic acid	12872.1 ± 2298.7	2862.6 ± 723.7	-78%	<0.0001	1.05
gluconic acid	2267.3 ± 287.2	477.9 ± 87.7	-79%	<0.0001	1.12
ethylsuccinate	2665.6 ± 378.4	552.9 ± 97.6	-79%	<0.0001	1.21
alpha tocopherol	45003 ± 6800.2	7962.4 ± 491.4	-82%	<0.0001	1.19
pantothenic acid	2542.9 ± 353.9	415.9 ± 97.6	-84%	<0.0001	1.21
behenic acid	52647.5 ± 8780	8593.8 ± 881.2	-84%	<0.0001	1.22
benzoic acid	12287.6 ± 1546	1978.5 ± 332.4	-84%	<0.0001	1.26
azelaic acid	2848.2 ± 423.4	428.4 ± 48.8	-85%	<0.0001	1.13
pelargonic acid	22382.1 ± 3025.4	3253.7 ± 891.9	-85%	<0.0001	1.25
glycolic acid	50511.1 ± 8802.1	6922.8 ± 709.6	-86%	<0.0001	1.16
2-hydroxyglutaric acid	7370.1 ± 1423.2	996.8 ± 250.2	-86%	<0.0001	1.22
sulfuric acid	2176.6 ± 447.9	285.2 ± 46	-87%	<0.0001	1.14
methanolphosphate	1676.1 ± 282.6	218.4 ± 28.6	-87%	<0.0001	1.23
glycerol	118868.5 ± 29459.2	13476.8 ± 2562.8	-89%	<0.0001	1.20

[1] Values are means ± SEM, n = 9 per group. Selected metabolites are annotated metabolites that had mean bootstrapped variable importance in projection (VIP) measurements ≥ 1 and bootstrapped variable importance in projection (VIP) measurements ≥ 1 and significant group differeneces after false discovery rate (FDR) correction. For sake of brevity, non-annotated metabolites are not presented, but are provided in supplementary table S2.

[2] Group comparisons assessed by Mann Whitney U tests. P-value has been adjusted for FDR correction. Statistical significance set at Padj ≤ 0.05.

[3] VIP calculated from bootstrapped partial least squares-discriminant analysis (PLS-DA) models derived from training data (n = 6 animals per group).

TABLE 3: Serum metabolite characteristics of male rats with chronic kidney disease fed a low-fiber or HAMRS2 supplemented diet.[1]

Serum

Metabolite	CKD-Low Fiber Mean ± SEM	CKD-HAMRS2 Mean ± SEM	Percent Change	*P* [2]	VIP[3]
Nitrogenous Metabolites					
indole-3-acetate	185.4 ± 12.1	1325 ± 122.5	615%	<0.0001	1.98
indole-3-lactate	320.1 ± 41.2	752.9 ± 105.1	135%	0.045	1.52
thymidine	3468 ± 80.1	2797.7 ± 86.6	-19%	<0.0001	1.67
cytosine	1106 ± 47.1	800.6 ± 65.1	-28%	0.02	1.37
uric acid	1389.8 ± 81	878.7 ± 50.7	-37%	<0.0001	1.65
Carbohydrates					
erythritol	1029.8 ± 101	2288.2 ± 309.8	122%	<0.0001	1.69
xylitol	593.7 ± 58.9	1157.2 ± 139.1	95%	0.045	1.52
threonic acid	2234.3 ± 122.8	3060.1 ± 191.3	37%	0.045	1.30
1,5-anhydroglucitol	16524.3 ± 1147.7	11231.1 ± 704.1	-32%	0.035	1.61
Other Metabolites					
malic acid	414.7 ± 26.6	777.1 ± 53.7	87%	<0.0001	1.68
β-hydroxybutyric acid	8938.1 ± 879.2	14936.8 ± 1466.2	67%	0.02	1.44
fumaric acid	265 ± 15.3	401.2 ± 29.8	51%	0.02	1.40

[1] Values are means ± SEM, n = 9 per group. Selected metabolites are annotated metabolites that had mean bootstrapped variable importance in projection (VIP) measurements ≥ 1 and bootstrapped variable importance in projection (VIP) measurements ≥ 1 and significant group differeneces after false discovery rate (FDR) correction. For sake of brevity, non-annotated metabolites are not presented, but are provided in supplementary table S2.

[2] Group comparisons assessed by Mann Whitney U tests. P-value has been adjusted for FDR correction. Statistical significance set at Padj ≤ 0.05.

[3] VIP calculated from bootstrapped partial least squares-discriminant analysis (PLS-DA) models derived from training data (n = 6 animals per group).

TABLE 4: Urine metabolite characteristics of male rats with chronic kidney disease fed a low-fiber or HAMRS2 supplemented diet.[1]

Urine

Metabolite	CKD-Low Fiber Mean ± SEM	CKD-HAMRS2 Mean ± SEM	Percent Change	*P*[2]	VIP[3]
Amino Acids					
taurine	11165.6 ± 2015.9	44428.1 ± 10799.	298%	0.002	1.22
tyrosine	4618.8 ± 357.4	7810.4 ± 879.4	69%	0.011	1.20
isoleucine	955.7 ± 63.6	1566.3 ± 156.9	64%	0.027	1.00
alanine	8575.8 ± 827.1	13386.2 ± 1104.6	56%	0.009	1.18
Other Nitrogenous Metabolites					
pantothenic acid	359.7 ± 58.6	933.4 ± 95.4	159%	0.002	1.33
furoylglycine	1208 ± 169.7	2377.6 ± 270.4	97%	0.022	1.19
creatinine	19434.2 ± 2430	35627 ± 3013.7	83%	0.011	1.41
isothreonic acid	3736.1 ± 330.1	6228.2 ± 420.1	67%	0.004	1.44
pseudo uridine	25851.9 ± 2184.4	42166 ± 3476.7	63%	0.008	1.35
oxoproline	15061.7 ± 1181	21692.2 ± 1730	44%	0.014	1.13
p-cresol	182951.3 ± 13963.6	96566.9 ± 21254	-47%	0.017	1.08
4-pyridoxic acid	406.9 ± 23.3	214.2 ± 15.4	-47%	0.001	1.46
indole-3-lactate	1045 ± 113.1	473.6 ± 52.7	-55%	0.005	1.25
methionine sulfoxide	2984.9 ± 220.4	1270.1 ± 133.6	-57%	0.001	1.43
indoxyl sulfate	3955 ± 517.4	1357.9 ± 116	-66%	0.002	1.23
hydroxylamine	13658.7 ± 1759.4	4623.3 ± 1614	-66%	0.009	1.27
hippuric acid	37300.9 ± 5689.2	9868.6 ± 1130.4	-74%	0.001	1.43
2,8-dihydroxyquinoline	3870.6 ± 466.5	619.7 ± 85.4	-84%	0.001	1.48
Lipids					
heptadecanoic acid	2625.7 ± 349	1494.4 ± 296.2	-43%	0.027	1.03
palmitic acid	27796.3 ± 3393.8	14969.3 ± 3104.1	-46%	0.017	1.02
myristic acid	6624.2 ± 720.8	3521 ± 735.1	-47%	0.014	1.03
caprylic acid	2837.8 ± 189.4	1454.4 ± 300.2	-49%	0.009	1.07
pelargonic acid	8742.8 ± 1092.4	4334.6 ± 1250.2	-50%	0.027	1.09
capric acid	1062.1 ± 131.9	301.1 ± 71.8	-72%	0.002	1.25
Carbohydrates					
sucrose	2818 ± 490.3	12824.6 ± 1849.4	355%	0.001	1.41
inulotriose	509.1 ± 55.9	1875.4 ± 307.6	268%	0.001	1.38
levoglucosan	661 ± 44.5	2208.6 ± 159	234%	0.001	1.53
maltose	76813.1 ± 18249.1	196750.6 ± 3332(	156%	0.014	1.23
xylitol	2024 ± 200.5	4067.7 ± 649.4	101%	0.009	1.25
fucose	9950.4 ± 700	17077.6 ± 1361.1	72%	0.004	1.39
erythritol	10914 ± 944.7	18329.7 ± 1329.5	68%	0.006	1.45
ribose	906.2 ± 43.4	1253.4 ± 107.7	38%	0.032	1.01
threitol	1411.7 ± 126.1	1872 ± 109.1	33%	0.04	1.19
digalacturonic acid	516.8 ± 37.4	265.4 ± 46	-49%	0.009	1.14
Other Metabolites					
tartaric acid	9574.2 ± 2039.6	92107.6 ± 11429.4	862%	0.001	1.53

isocitric acid	4551 ± 364.7	7746.3 ± 838.8	70%	0.017	1.30
ribonic acid	1392.2 ± 166.1	2211 ± 226.8	59%	0.022	1.14
aconitic acid	2150.7 ± 174.7	3162.9 ± 350.7	47%	0.032	1.14
pyruvic acid	443.6 ± 47.4	286.8 ± 35.5	-35%	0.04	1.01
glycolic acid	1799.8 ± 160.7	1119.6 ± 134.1	-38%	0.014	1.08
azelaic acid	408.1 ± 57.2	204.3 ± 54.2	-50%	0.032	1.16
benzoic acid	7514.4 ± 679.2	3506.1 ± 797	-53%	0.011	1.11
ferulic acid	457.4 ± 57	200.9 ± 36.7	-56%	0.004	1.08
3-hydroxyphenylacetic acid	583.4 ± 41.1	210.8 ± 36.4	-64%	0.001	1.46
phenol	5549.9 ± 779.2	1445.2 ± 239.8	-74%	0.001	1.32
3-(3-hydroxyphenyl)propionic acid	3547.2 ± 870.4	560.4 ± 63.6	-84%	0.004	1.36
glycerol-3-galactoside	7002.1 ± 557.6	913.3 ± 88.7	-87%	0.001	1.51

[1] Values are means ± SEM, n = 9 per group. Selected metabolites are annotated metabolites that had mean bootstrapped variable importance in projection (VIP) measurements ≥ 1 and bootstrapped variable importance in projection (VIP) measurements ≥ 1 and significant group differeneces after false discovery rate (FDR) correction. For sake of brevity, non-annotated metabolites are not presented, but are provided in supplementary table S2.

[2] Group comparisons assessed by Mann Whitney U tests. P-value has been adjusted for FDR correction. Statistical significance set at Padj ≤ 0.05.

[3] VIP calculated from bootstrapped partial least squares-discriminant analysis (PLS-DA) models derived from training data (n = 6 animals per group).

TABLE 5. Percent changes in uremic retention solutes in cecal contents, serum , and urine in male CKD rats fed HAMRS2 relative to low fiber-fed CKD controls[1]

Metabolite	Cecal Contents	Serum	Urine
Nitrogenous Metabolites			
creatinine	**-52.5% ***	**-13.4%**	**83.3% ***
hippuric acid	**N.R.**	**N.R.**	**-73.5% ***
indole-3-acetate	**-12.1%**	**614.7% ***	**-2.6%**
indole-3-lactate	**-71.7% ***	**135.2% ***	**-57.4% ***
indoxyl sulfate	**N.R.**	**-36.0%**	**-65.7% ***
p-cresol	**N.R.**	**N.R.**	**-47.2% ***
putrescine	**57.9%**	**N.R.**	**-20.4%**
spermidine	**-70.7%**	**N.R.**	**-32.6% §**
urea	**-79.0% ***	**-0.3%**	**-15.4%**
uric acid	**-85.1% ***	**-36.8% ***	**51.1% §**
Polyols			
erythritol	**26.9%**	**122.2% ***	**67.9% ***
mannitol	**245.5%**	**-27.9% §**	**-1.3%**
myo-inositol	**-83.3% ***	**5.50%**	**17.8%**
Other			
phenol	**-74.1% ***	**N.R.**	**-74.0 ***

[1] N.R. metabolite not reported by GC-TOF-MS. Metabolites that were featured in partial least squares-discriminant models are denoted with an *. Metabolites that were significantly different (Mann Whitney U test) before false discovery rate (FDR) correction are denoted with a §.

Summary of Metabolite Changes

Cecum	Serum	Urine
465 identified metabolites 256 metabolites significantly different • 109 metabolites annotated **Main Findings:** Nitrogenous metabolites reduced in HAMRS2 group: • Branched-chain amino acids • Lysine, methionine, phenylalanine, serine and proline derivative • Purine catabolites (inosine, uric acid, xanthine) • Urea	300 identified metabolites 20 metabolites significantly different • 12 metabolites annotated **Main Findings:** Nitrogenous metabolites reduced in HAMRS2 group: • indole-3-acetate, indole-3-lactate • Uric acid	276 identified metabolites 114 metabolites significantly different • 47 metabolites annotated **Main Findings:** Nitrogenous metabolites reduced in HAMRS2 group: • Alanine, isoleucine, taurine, tyrosine • Creatinine, indole-3-lactate, indoxyl sulfate, *p*-cresol
Lipid metabolites reduced in HAMRS2 group: • Capric acid (C10) • Lauric acid (C12) • Myristic acid (C14) • Palmitic acid (C16) • Heptadecanoic acid (C17) • Isoheptadecanoic acid • Stearic acid (C18) • Linoleic acid (C18:2) • Nonadecanoic acid (C19)	No difference in measured lipid metabolites between groups	Lipid metabolites reduced in HAMRS2 group: • Caprylic acid (C8) • Pelargonic acid (C9) • Capric acid (C10) • Myristic acid (C14) • Palmitic acid (C16) • Heptadecanoic acid (C17)
Carbohydrate metabolites greater in HAMRS2 group: • Lactose, maltose	Carbohydrate metabolites greater in HAMRS2 group • Erythritol, xylitol	Carbohydrate metabolites greater in HAMRS2 group • Erythritol, maltose, sucrose
Carbohydrate metabolites reduced in HAMRS2 group: • Sugar alcohols: 1,5-anhydroglucitol, myo-inositol, xylitol	Carbohydrate metabolites reduced in HAMRS2 group • 1,5-anhydroglucitol	
	Other metabolites greater in HAMRS group • Organic acids: fumaric acid, malic acid • Ketone body: β-hydroxybutyric acid	Other metabolites reduced in HAMRS2 group • Organic acids: pyruvic acid • Phenol